VOLUME II-1

THE NATURAL ENVIRONMENT NEAR SAN ONOFRE

DRAFT FINAL REPORT 1987

PHYSICAL/CHEMICAL OCEANOGRAPHY PROGRAM
AT SONGS

Submitted to: Marine Review Committee
531 Encinitas Blvd., #105
Encinitas, CA 92024

Submitted by: John Reitzel
Hany Elwany
Karel Zabloudil
M. Rustin Erdman
Principal Investigators

ECOSystems Management Assoc., Inc.
531 Encinitas Blvd., Suite 119
Encinitas, CA 92024

January 20, 1988

VOLUME II-1

THE NATURAL ENVIRONMENT NEAR SAN ONOFRE

TABLE OF CONTENTS

VOLUME II-2

THE NATURAL ENVIRONMENT NEAR SAN ONOFRE

1. INTRODUCTION

A great part of MRC's program is to assess SONGS' effect on marine populations. This requires monitoring and study of the physical/chemical conditions off San Onofre in order to provide an explanation of the biological changes, natural or SONGS induced, in terms of observed physical changes and known biophysical mechanisms.

This report is oriented towards providing a review of the natural events which occurred during the period of the study. As will be shown here, there were changes in the natural environment from year to year. The changes are more pronounced during the El Nino period, August 1982 to July 1984, which brought continued high temperatures and depletion of nutrients to coastal water off San Onofre. The 1982-84 El Nino was also associated with severe winter storm waves which caused disturbance to the sea bottom. The 1982-84 El Nino is probably the largest major event during this study. Since El Nino is a very large-scale event, it has about the same overall effect on the entire area of the study.

Section 2 gives the geographic location of San Onofre, the description of the study site, and the location of the major kelp beds and creeks in the area. The data used in this report are discussed in Section 3.

Section 4 presents the oceanographic conditions off San Onofre from 1981-1986, to give an account of the natural events. It is intended to provide both overall interpretation of the events and enough detail to examine the physical/chemical conditions for comparison at specific times and places with the biological samplings.

A summary of the major oceanographic events between 1981 through 1986 is given in Section 5.

2. DESCRIPTION OF THE SITE

San Onofre Nuclear Power Station is located halfway between San Diego and Los Angeles at the edge of a roughly 6-10 kilometer wide continental shelf. Figure 2-1 shows a large regional map of the study site where San Onofre is at 117° 33' 25" longitude and 33° 22' 12" latitude.

Figure 2-2 is a more detailed map of the study region. It shows an area of 18 x 9 km at SONGS revealing the bathymetry and the location of the intakes and outfalls for the three units. All three intakes are located in about 8 meters of water, 3 meters off the bottom. Unit 1 uses a point discharge while Units 2 and 3 incorporate staged diffusers to disperse the once-through sea water used in the secondary cooling systems. Note the protrusion of San Mateo Point onto a locally narrowing shelf. This is the largest irregularity in the coastline and nearshore bathymetry for 10 km up or down the coast. San Onofre beach is indicated in Figure 2-2 as one of the possible areas of SONGS' impact. Figure 2-2 also shows the major cobble substrates which present areas of potential kelp habitation (see Vol IV-2 for more detail), and the major creeks in the study area.

The major kelp beds in the area are San Mateo kelp, San Onofre kelp and Barn kelp. These beds are primarily inhabited by the giant kelp Macrocystis pyrifera and provide a rich habitat for several species of fish, invertebrates and algae.

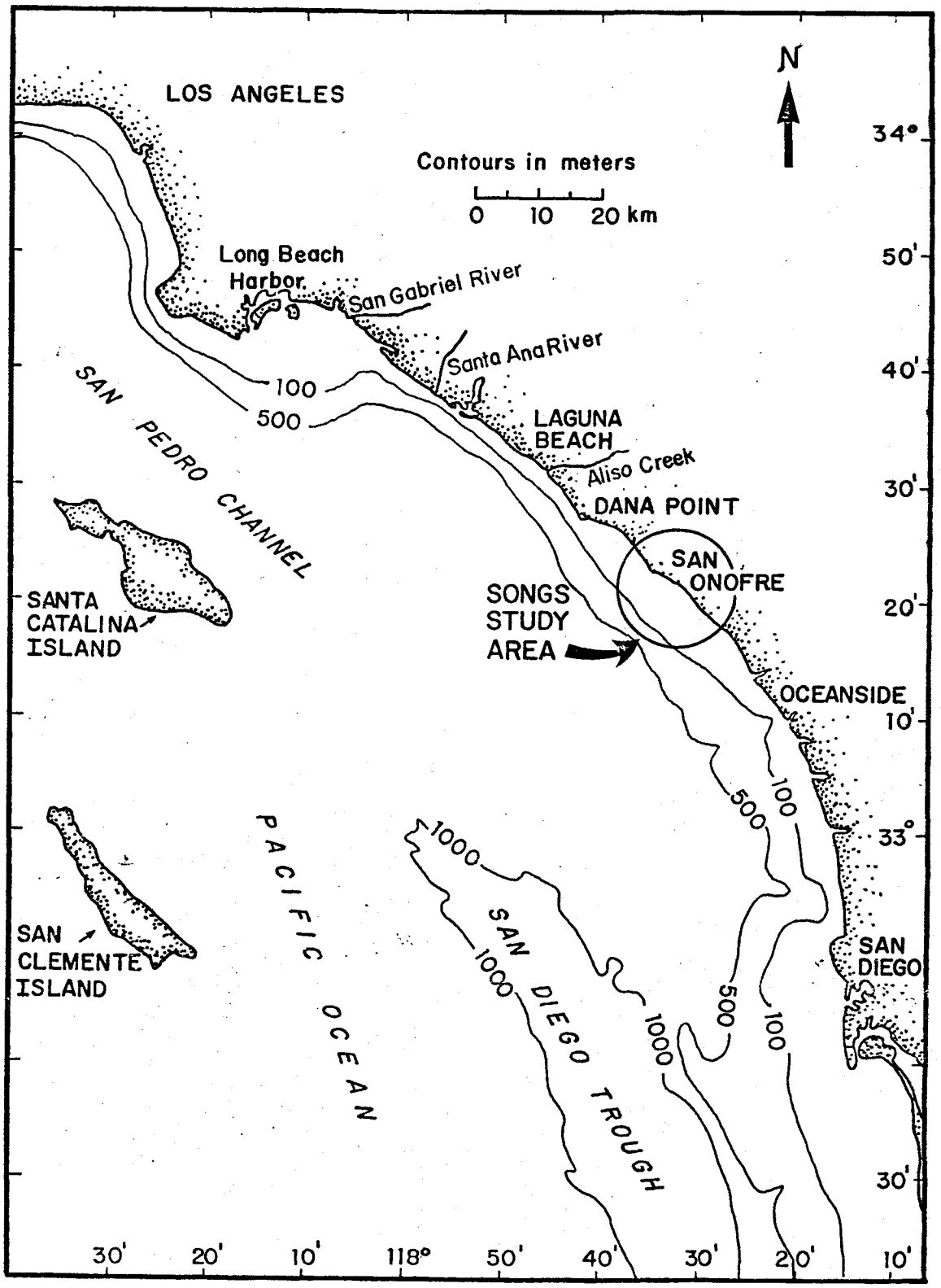

Figure 2-1. Regional map of the study site

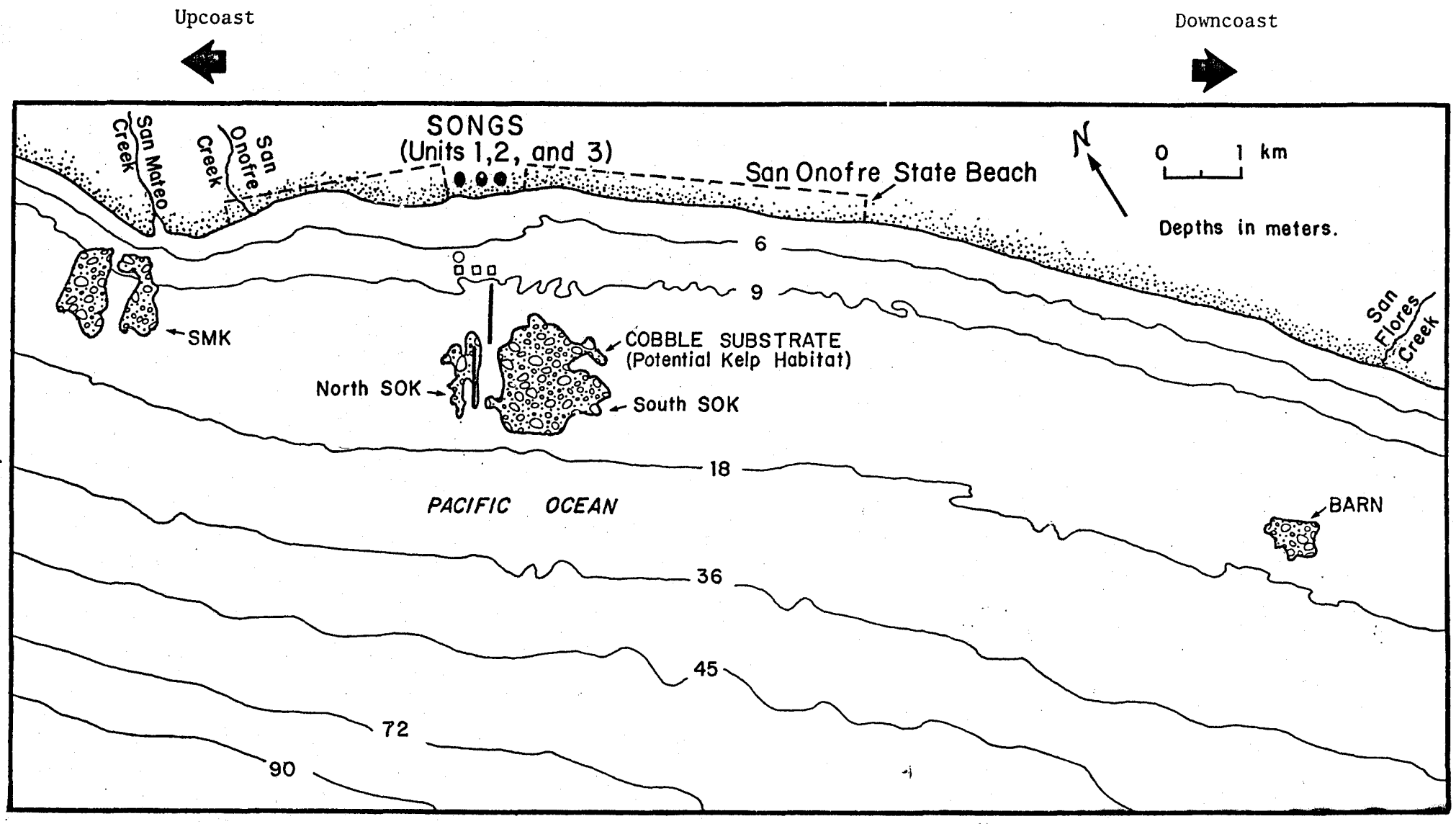

Figure 2-2. Detailed map of the study site

□ = UNITS 1,2,& 3 INTAKES
O = UNIT 1 DISCHARGE
—— = DIFFUSER LINES

For the analyses of the continuous data of temperature and irradiance measurements, we have chosen to show our results from stations SMK45 and SOK45. The latter station is constructed by averaging the hourly measurements from SOKU45 and SOKD45. This is designed to represent time series with as few data graphs as possible. SOKU45 and SOKD45 are located in the vicinity of the San Onofre kelp bed and SMK45 is located in the San Mateo kelp bed. Both stations are in a total water depth of 14 meters.

4. OCEANOGRAPHIC CONDITIONS

4.1. Temperature and Nutrients

The coastal waters off San Onofre over the last ten years have been temperate: surface temperature in late summer is typically near 20°C (68°F), with a maximum near 25°C (77°F); winter surface temperature is typically near 15°C (57°F). At a depth of 14 m, temperatures around 15°C are typically found in any season. Table 4-1 shows the basic statistics of bottom temperature at stations SMK45 and SOK45 for various seasons and years. This table gives the mean, standard deviation (STD), maximum (max), minimum (min) temperatures, and number of days used in the calculations (N).

Apart from its direct effect on biochemical processes, temperature has strong indirect influence on the conditions of life in the sea. One of the most important is the effect of temperature stratification on the availability of nutrients in shallow coastal waters. The density of the ocean waters near SONGS varies mainly because of varying temperature. Vertical stratification of density, with warmer waters overlying colder, strongly inhibits vertical mixing because of the energy required to overcome the force of buoyancy. A large part of the dissolved nutrients used by plant life in the nearshore waters comes from a reservoir of nitrate and phosphate in deep waters, which only becomes available in shallow waters through vertical mixing or mass movements. Since plant life in the sea depends largely on bringing together light from above and dissolved nutrients from below, the limitation of vertical mixing by stratification of temperature may be critical.

Off San Onofre, the concentration of nitrate is low in waters greater than 14°C, and increases rapidly with decreasing temperature below 14°. The stratum in which nutrients increase rapidly with depth is called the nutricline. Taking nitrate as representative of other nutrients as well, the top of the nutricline near San Onofre is

TABLE 4-1

STATISTICS OF BOTTOM TEMPERATURE (C)

		SMK45					SOK45				
YEAR	SEASON	MEAN	STD	MAX	MIN	N	MEAN	STD	MAX	MIN	N
81-82	WINTER	14.7	1.2	17.9	12.5	142	14.5	1.1	18.4	12.9	140
82	SUMMER	14.5	1.9	19.9	11.6	128	15.1	2.0	20.5	11.8	183
82-83	WINTER	16.1	0.6	18.5	14.3	143	16.2	0.7	19.1	14.7	143
83	SUMMER	16.2	1.8	20.6	12.5	121	16.6	1.7	21.6	12.9	164
83-84	WINTER	16.1	2.0	20.9	12.8	182	16.1	2.0	20.9	13.4	181
84	SUMMER	16.8	1.7	23.4	12.8	162	17.3	2.0	23.1	12.0	175
84-85	WINTER	14.4	1.9	19.7	11.8	126	13.8	2.8	19.0	0.0	182
85	SUMMER	15.2	2.1	20.8	11.1	138	15.0	2.1	21.5	10.6	174
85-86	WINTER	14.9	1.0	18.1	12.7	176	15.3	1.3	19.3	13.5	181
86	SUMMER	14.0	1.7	18.3	10.7	180	14.6	2.2	20.5	11.1	183
86-87	WINTER	16.8	0.6	18.1	15.2	81	17.6	1.8	23.7	15.2	92

generally located close to the isothermal surface at 14°C, at whatever depth that may be. Figure 4-1 shows the relationship between nitrate and temperature. The theoretical relation of N-T is given by:

$$N = 4.065\ i^1\ \mathrm{erfc}\ \{(T-13.91)/1.16\}$$

where i^1 erfc is the first integral of the complementary error function. For further discussion on this relation, see Reitzel et al (1987, Vol. V-2).

The main agent of vertical mixing in the nearshore waters off San Onofre is the turbulence generated by wind stress on the surface and by bottom stress due to local currents. The main agent opposing vertical mixing is solar heating of the sea surface, setting up a density stratification that inhibits the vertical turbulence. Sometimes in mid winter the turbulence dominates and the nearshore water column is almost completely mixed, with the top only a small fraction of a degree Celsius warmer than the bottom. Commonly the top to-bottom difference in 14 m depth is about one degree in winter, rising in irregular steps during calm periods in spring to about five degrees in summer, and falling back in steps with autumn storms to its winter value.

Time histories of daily averages of surface and bottom temperatures are shown in Figures 4-2 and 4-3. They are plotted year by year, from 1981 through 1986, for the entire data set. These plots present daily means, from which the internal waves are effectively filtered out, and they show the detailed course of the onset and breakdown of stratification, upwelling and downwelling episodes, and the major changes in the El Nino years. As a useful rough index of nutrient availability in different seasons and years, the fraction of time below 14°C is a useful quantity to keep in mind while examining these histories.

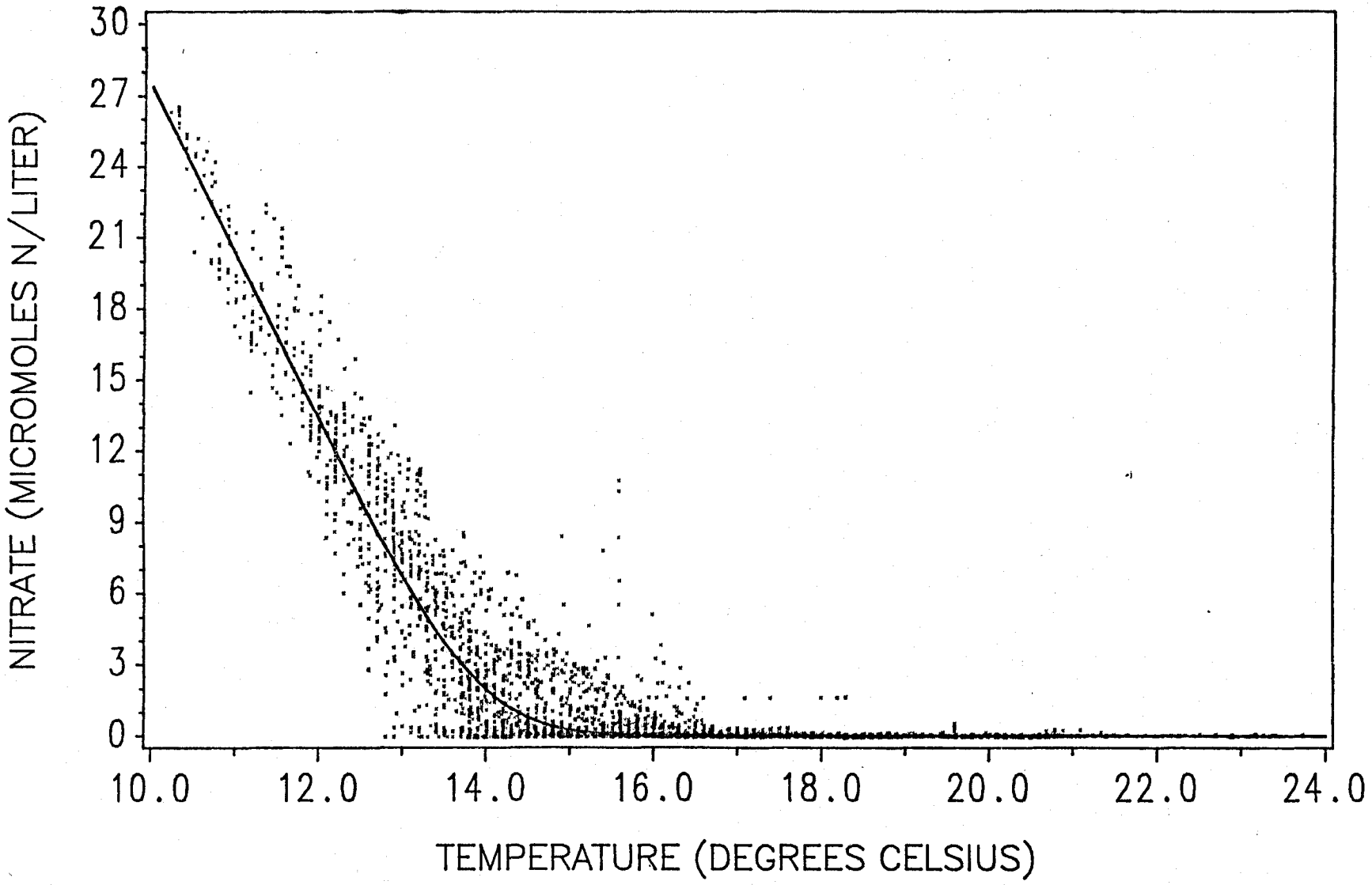

Figure 4-1. Measured nitrate versus temperature with the solid line representing the N - T relationship

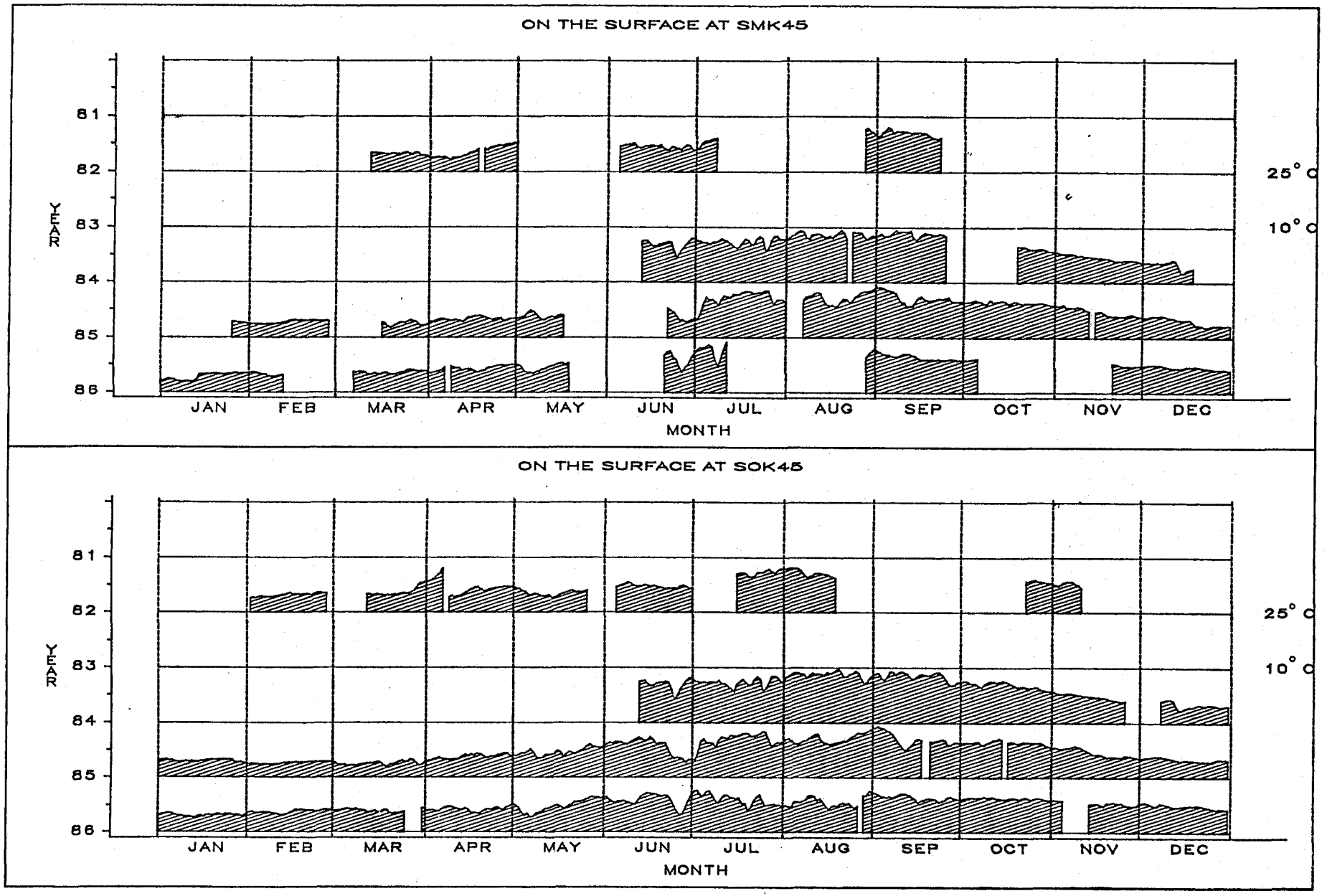

Figure 4-2: Time histories of daily mean surface temperatures

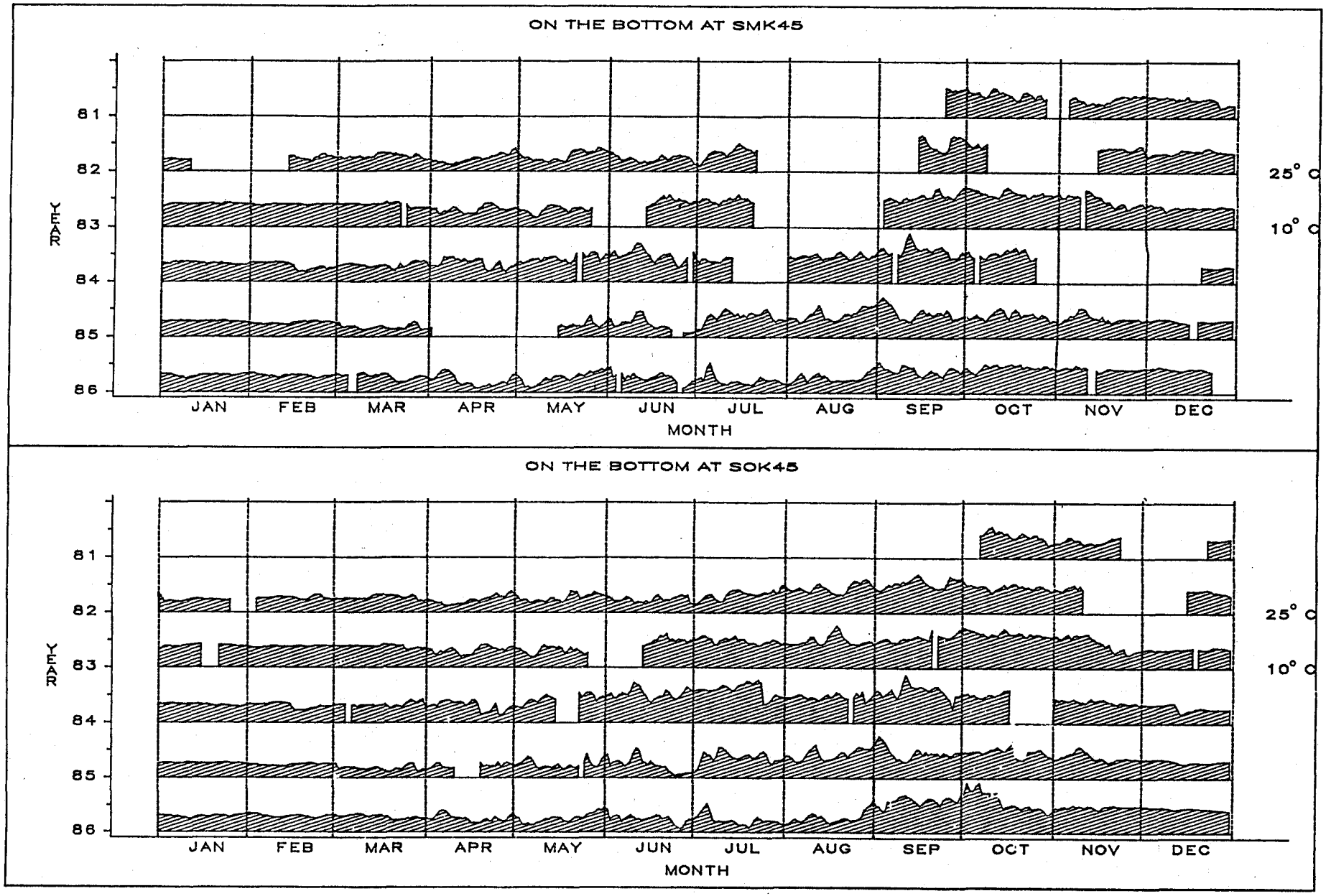

Figure 4-3. Time histories of daily mean bottom temperatures

The isopleths of temperature and nutrient versus depth at the inshore stations are displayed in Figures 4-4 and 4-5. They clearly show the distribution of these physical variables with depth. The change in the difference between surface and bottom temperature (ΔT) over various months can easily be seen in Figure 4-4.

4.1.1. Internal waves

Just as the interface between air and water at the sea surface is disturbed by waves, so are internal interfaces between density strata in the water column. More complicated but essentially similar waves occur in an overall density gradient without sharp interfaces. Internal waves off San Onofre may be as much as a few meters high, comparable to surface waves, but they have much smaller wave velocities (on the order of 10 cm/sec) and much longer periods, ranging from tens of minutes up to tidal periods of 1/2 day and one day. The most important are the tidal internal waves, which originate at the shelf break and advance toward the shore; these are active in summer when stratification is greatest.

As a result of internal waves, vertical profiles of water properties can change significantly from hour to hour; this should be kept in mind in interpreting measurements. Internal waves in nearshore waters can periodically raise the nutricline a few meters above its mean level, bringing nutrients closer to shore than they would otherwise reach. High internal waves can also break as they approach the shore, contributing to nearshore vertical mixing.

4.1.2. Upwellings and Downwellings

The velocities of currents near the shore off San Onofre, in total water depths of 20 m or less, are mainly controlled by a balance of bottom stress against surface slope or wind stress; as a result, velocities generally fall off with depth and approach zero near the bottom. The rotation of the earth accelerates moving water to the

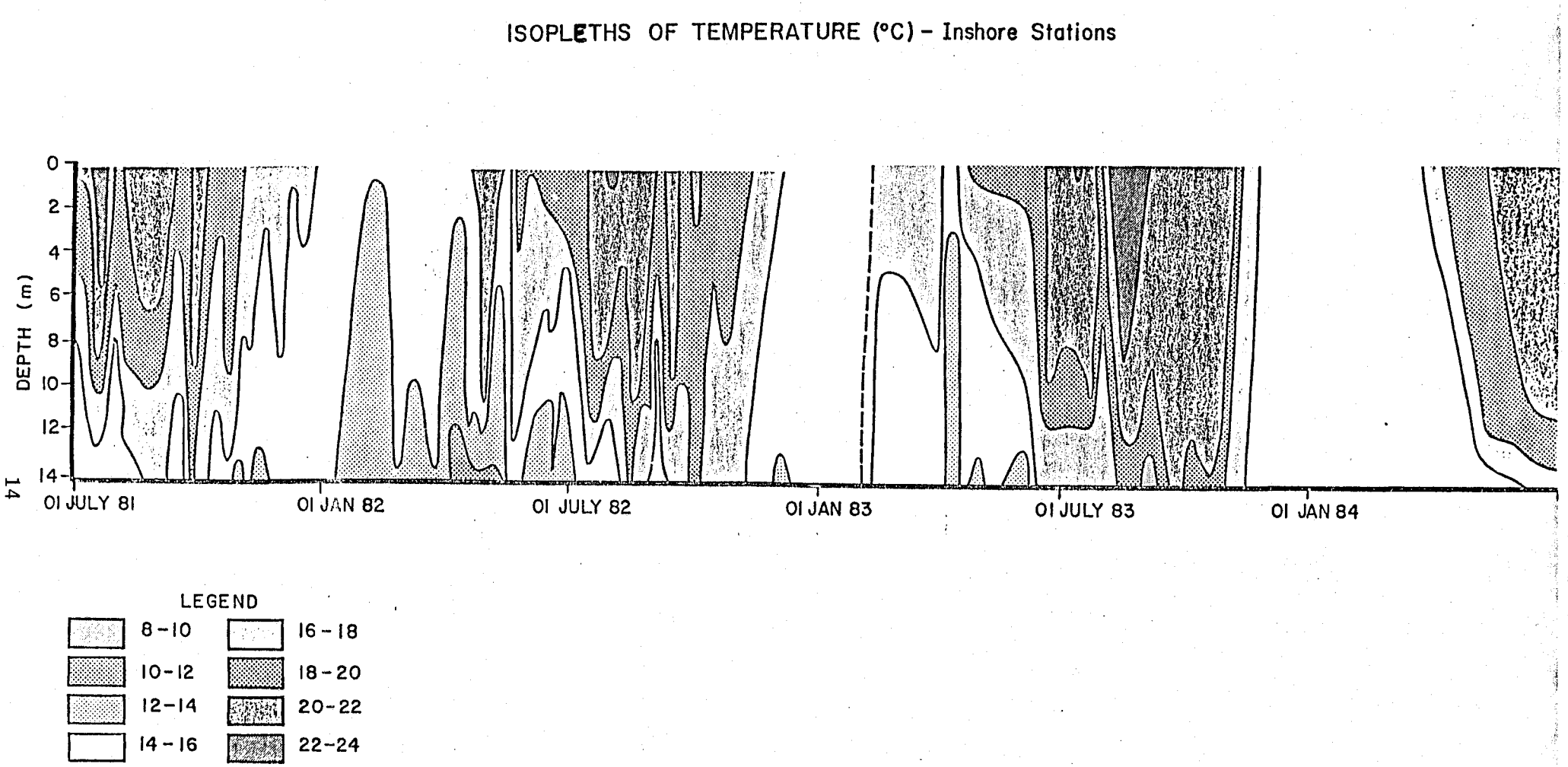

Figure 4-4. Isopleths of (NO3+NO2) versus depth over time. Data collected from stations at water depth less than 30 m. Units of (NO3+NO2) in micro moles/liter

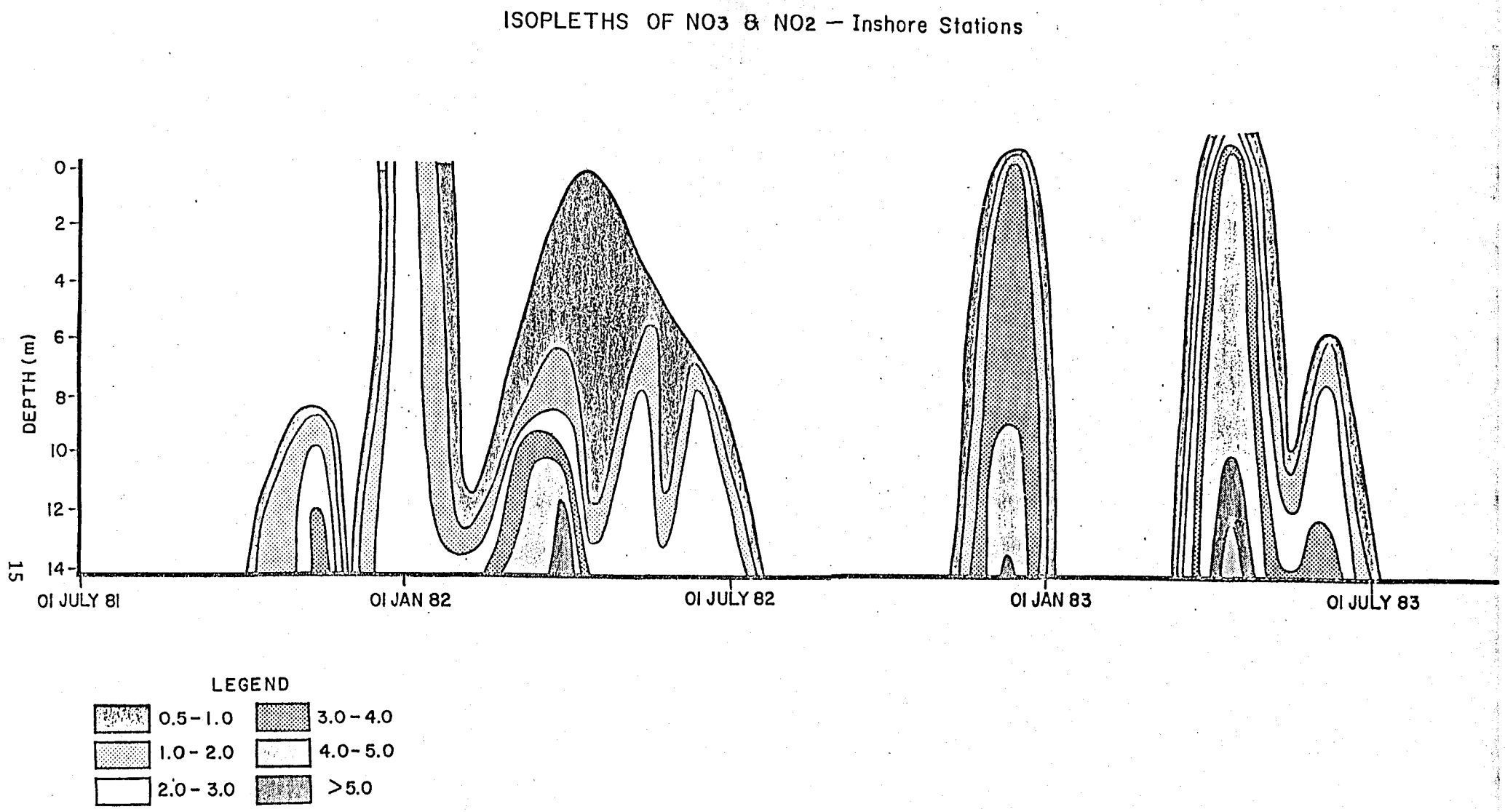

Figure 4-5. Isopleths of temperature versus depth over time. Data collected from stations at water depth less than 30 m.

right of its path in proportion to its velocity. The faster moving upper layers of a downcoast current will be more strongly accelerated offshore than the lower layers, producing an offshore flow of surface water which is replaced by an onshore flow of deeper water. This circulation would continue in uniform water, but when temperature and density are stratified a new balance can be struck with nearshore water colder than the water offshore at the same depth. Events of this sort are called upwellings, and are a principal means by which nutrients are brought into shallow nearshore waters. Events of the opposite kind, with upcoast currents leading to an accumulation of warm surface water near the shore, are called downwellings, and deprive the nearshore waters of nutrients. Major events take time to develop, and do not track current fluctuations faster than a day or two; the larger events generally do not last more than a week or ten days.

Upwellings off San Onofre become noticeable with the onset of stratification in March or April, as solar heating of the sea (including photosynthetic radiation) increases from its winter minimum. Upwellings that come close to the surface in shallow water may continue to occur through mid July, the season of maximum insolation, but are rare in late summer because strong downcoast winds are less frequent and the thicker layer of warm surface water is harder to break through. August and September, in fact, may be marked by nearshore downwellings in which the temperature at 14 m depth approaches 20°C.

4.1.3. El Nino

The occurrences of upwellings and downwellings are described above in very general terms because they may vary greatly from year to year, or over longer cycles of several years. The greatest interannual variability comes from El Nino events, which may affect a single season or extend over two successive years. The immediate cause of El Nino events is a slackening of the trade winds over the Pacific Ocean.

Normally the trade winds drive tropical surface water to the west, maintaining a thickened wedge of warm, clear, and nutrient poor water on the Asian side of the Pacific. If the winds slacken for several months or more, the water in this wedge flows eastward in a massive internal surge and piles up on the American side of the Pacific, raising mean sea level by as much as 10 or 20 cm, raising temperature by as much as 2 or 3°C, and submerging the nearshore nutricline to depths of several tens of meters. It is this depression of the nutricline which removes nutrients from the base of most marine food chains, with serious results for populations of marine fish and birds. The slackening of the trade winds also allows the westerly winds of the temperate zones to encroach on the tropics, causing unusually severe storms and rain on the west coasts of the Americas in lower latitudes.

The years of detailed oceanographic recording near SONGS extend from 1976 through 1986. In the middle of this period, and as SONGS Units 2 and 3 went from testing to full operation, an extreme El Nino event occurred, starting in the late summer of 1982 and lasting through the summer of 1984. This event was comparable to previous events in 1957-8, 1941-2, and 1914-15, indicating a mean recurrence interval of something over 20 years for such major events.

During the El Nino period (1982-84), several cruises were conducted. Data from these cruises are used here to identify the major changes in natural environment associated with the El Nino event. The data used here are from stations 30 to 100 m water depth, at 5 to 7 km offshore from the shoreline.

Figures 4-6 through 4-8 present isopleths of the following variables: NO3 + NO2 versus depth over time, NO_3 + NO_2 versus temperature over time, temperature versus depth over time, and salinity versus depth over time. These plots are a composite of data taken at several stations in the study area. The contours are drawn to minimize gradients and without reference to other data in order to

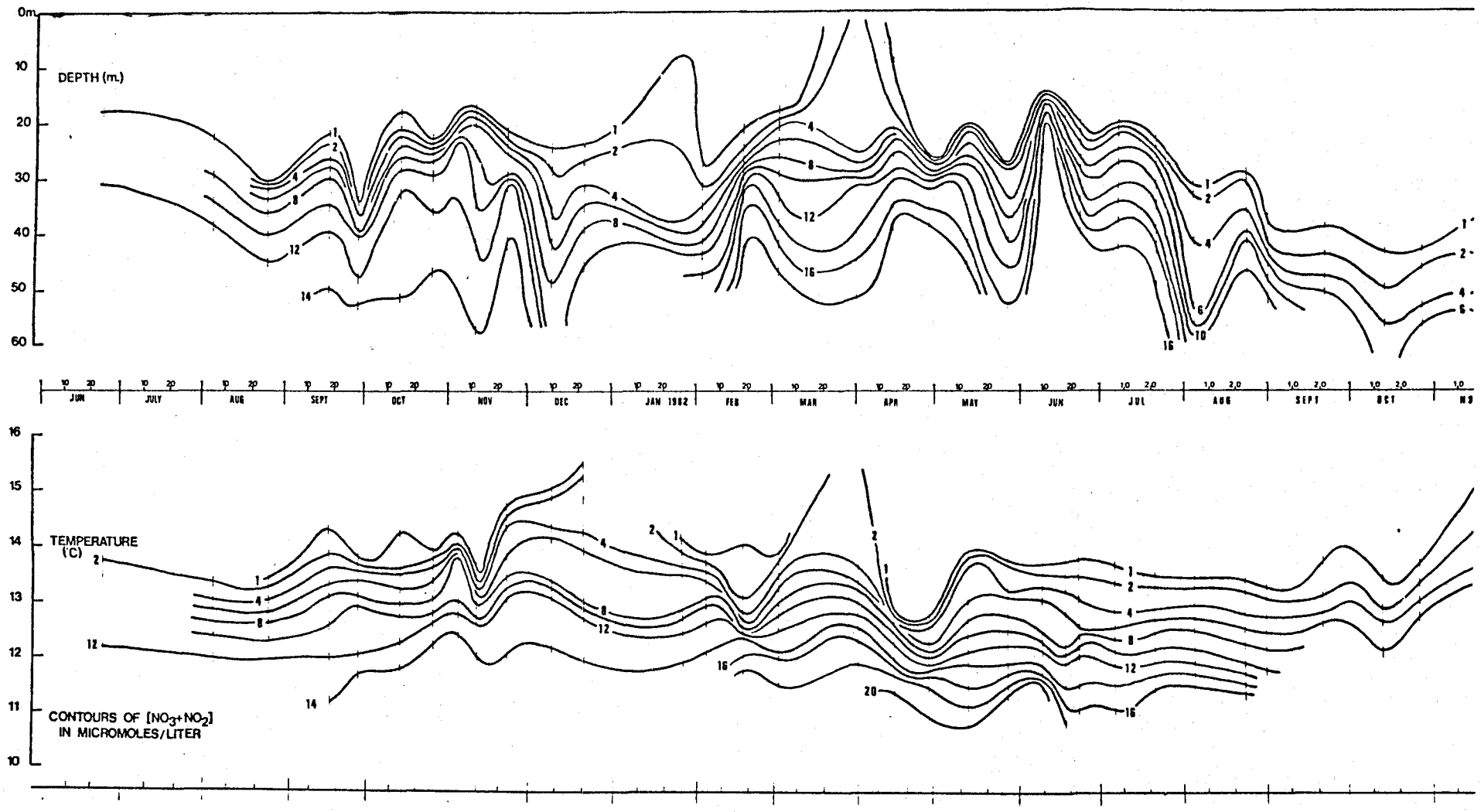

Figure 4-6a. Isopleths of (NO3+NO2) versus depth and temperature over time for offshore stations, 5 km offshore

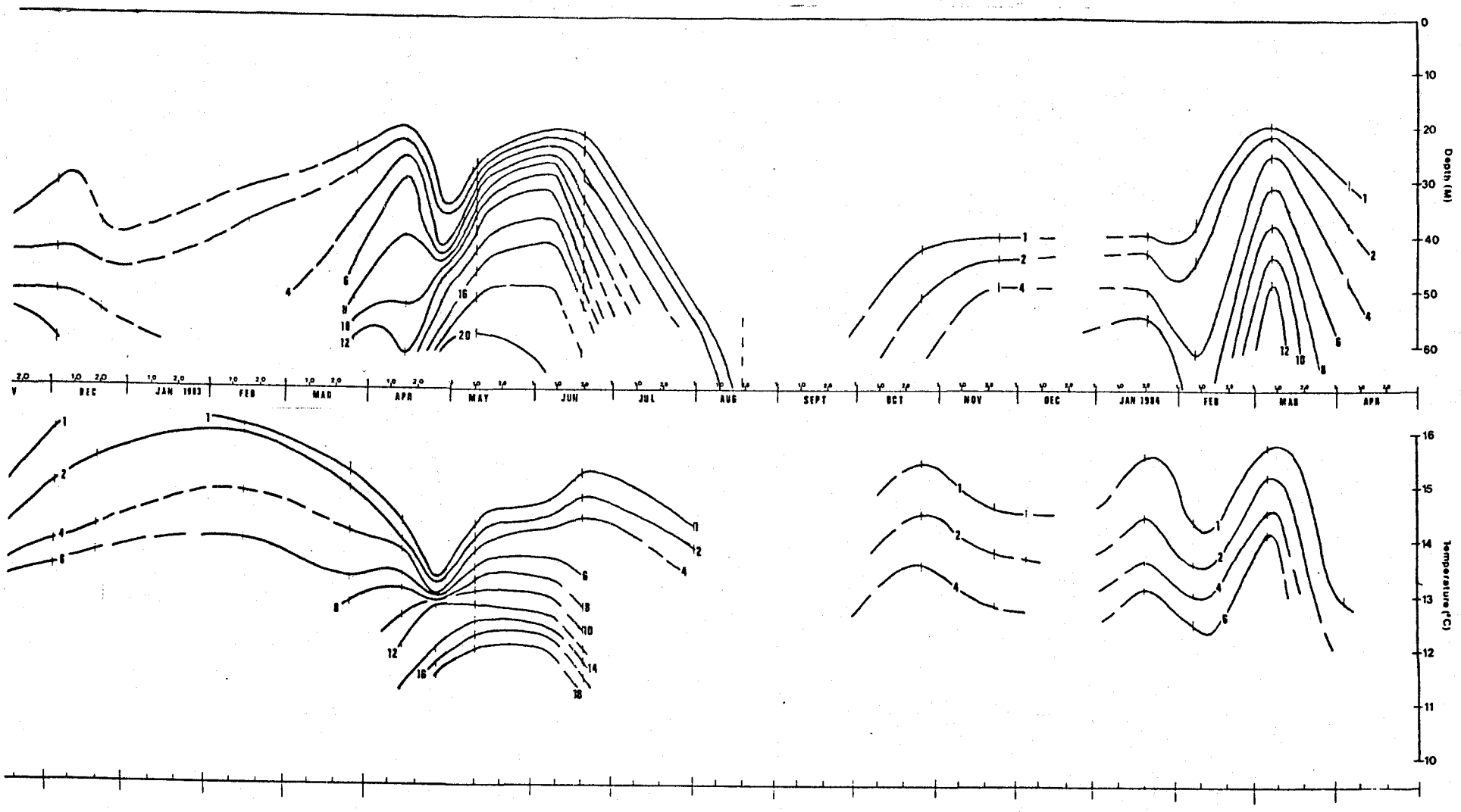

Figure 4-6b. Isopleths of (NO3+NO2) versus depth and temperature over time for offshore stations, 5 km offshore

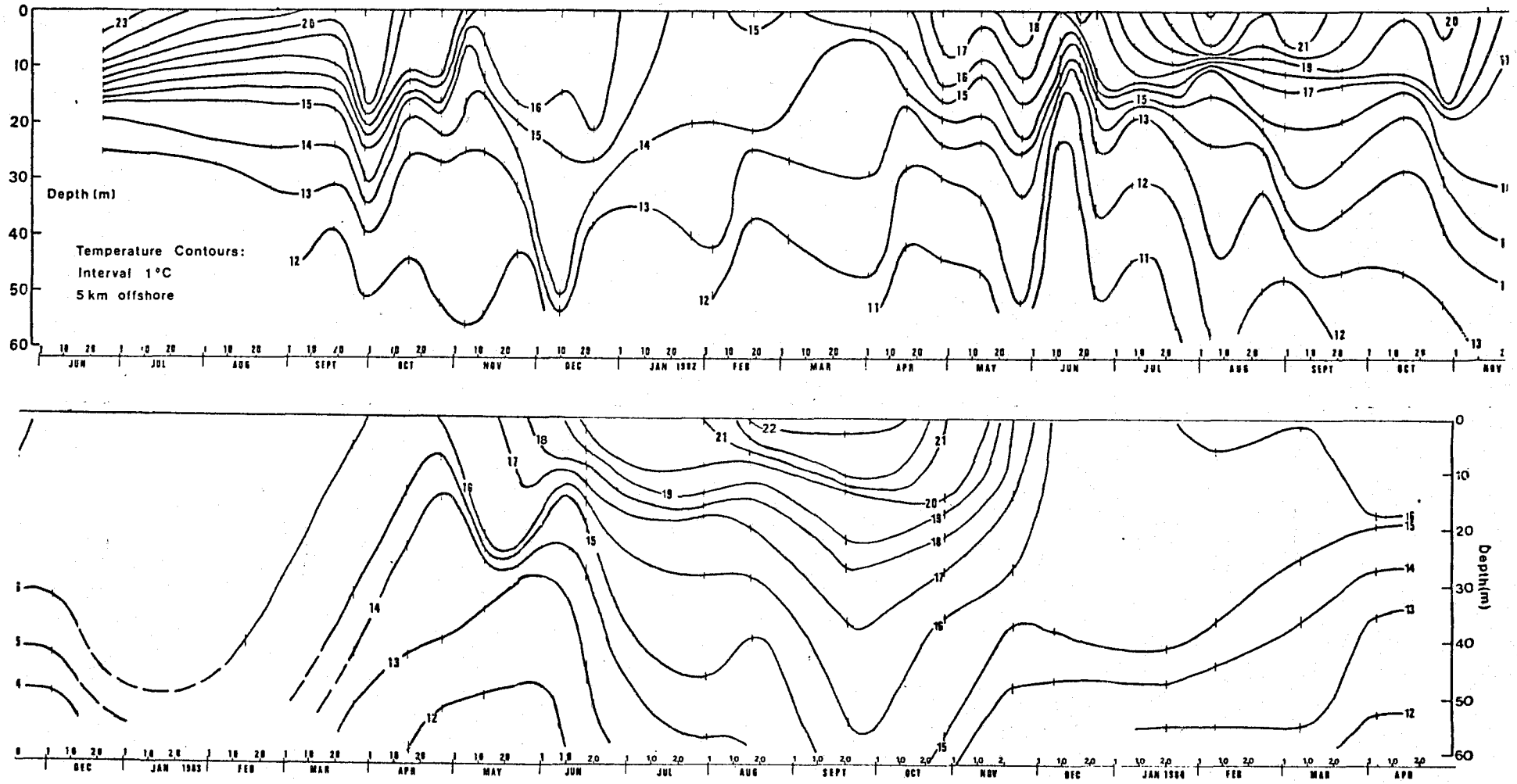

Figure 4-7. Isopleths of temperature (°C) versus depth over time for offshore stations, 5 km offshore

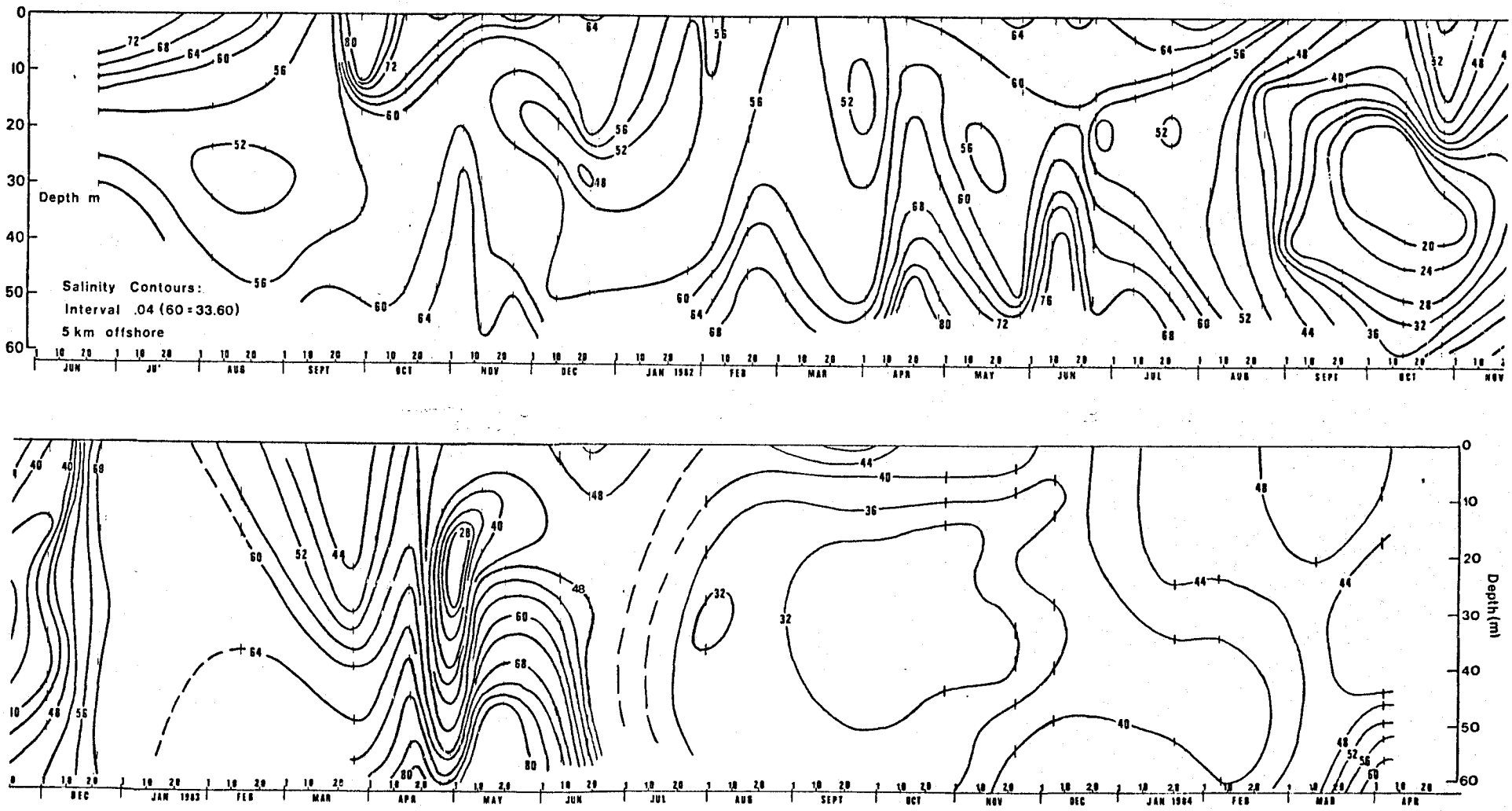

Figure 4-8. Isopleths of salinity versus depth over time for offshore stations, 5 km offshore

avoid interpretative contouring as much as possible. The cruise dates are shown by ticks on the contours. When no data is available, we extended the contours by a dotted line to show the general trends.

The following is an interpretation of this data:

1. El Nino appeared in September 1982 with the arrival of a water mass at 13-16°C and a low salinity of 33.20 which depressed the top of the nutricline to 30 m. This water came from about 500 km offshore from the west-southwest (see Calcafi Atlas #30, Lynn et al 1982).

2. In December 1982, this mass was replaced by a very homogeneous mass at 16-17°C with salinity of 33.60 (see Figure 4-8).

3. Temperature fell by 1° to 2°C in March 1983. Strong winds blowing downcoast in late March and early April, 1983, produced an upwelling that brought the nutricline up to 20 m and led to a phytoplankton bloom. By mid-April, winds blowing onshore and upcoast caused downwelling with a brief return of low salinity water, below 33.30.

4. Another upwelling at the end of May raised the nutricline again to about 20 m (now at the unusually high temperature of 14.5°C), where it remained through May and early June, when a second bloom may have occurred. Salinity was above 35.45 throughout this time.

5. During June and July, a thick mid-water mass reestablished itself below the summer thermocline, at 14-17°C with salinity about 33.35, and the nutricline gradually fell to below 30 m again. This return of El Nino conditions intensified through the next two months. By mid-September, the nutricline was down to 60 m, where the temperature was just below 16°C, and midwater salinity was again down to 33.30. Conditions remained about the same through the end of November, when the nutricline was still a little below 40 m and mid-water salinity below 33.40. This was the state until the end of 1983.

6. The decline of El Nino occurred in early 1984. By summer, El Nino was virtually over.

Minor El Nino events are also recognizable, recurring on the average about once in every 5 years. One such event began late in 1986, with temperatures at depths of 14 m remaining above 16°C through the end of the year.

4.2. Irradiance, Extinction, and Seston

The intensity of sunlight in the sea falls off exponentially with depth: that is, it decreases by a fraction of itself with each meter of increasing depth. The fraction of light lost per meter of depth is called the extinction coefficient K (m^{-1}), or simply the extinction; it depends a little on the diffuseness of the light, but mainly on the absorptive properties of the water and of the dissolved and suspended material in it. Other optical properties of the water such as turbidity and beam attenuation coefficient depend also on scattering, and do not reliably measure the actual decrease of intensity with depth.

The measure of light intensity used in this work is called irradiance, which is short for downwelling planar quantum irradiance of photosynthetically active radiation. This is the integral over all downward directions of the downward component of radiant energy flux in the waveband 400 to 700 nanometers, measured with a detector whose sensitivity is proportional to wavelength. Since the energy of a photon is inversely proportional to its wavelength, this measure effectively counts the photons reaching the detector per unit of time; the units of irradiance are Einsteins per square meter per day (E/m^2 day), or the equivalents for other time intervals. One Einstein represents one mole of photons available for photochemical reactions.

At San Onofre, the daily irradiance at the sea surface, averaged over daylight and dark hours, is generally about 50 E/m^2 day in

midsummer and about 20 E/m^2-day in midwinter (see Figure 4-9). The extinction in the local nearshore waters is highly variable, going from a minimum of about 0.1 m^{-1} to about 1 m^{-1}; values between 0.25 and 0.4 m^{-1} are commonly observed in all seasons. With a surface irradiance of 33 E/m^2 day, the underwater irradiance at 14 m depth will be close to 1.0 E/m^2 day when extinction is 0.25 m^{-1}, and about 0.12 E/m^2 day when extinction is 0.4 m^{-1}. This range from about .1 to 1 E/m^2 day is the range in which the growth and reproduction of marine plants may be limited by availability of light, depending on the species in question and on other factors. The sea bottom at 14 m depth off San Onofre is thus a more or less marginal environment for marine plants, whose success will depend on the vagaries of the local extinction coefficient.

The amount of blue light, in the range 400 to 520 nanometers, may be a limiting factor in gametogenesis of marine algae. From 117 days of direct comparison of blue and total quantum irradiance at 13.7 m depth, the ratio R of blue irradiance to the total was fitted to the relation $R = .31\ I^{.17}$ with $r^2 = .91$, giving R = .35 for I = 2 E/m^2 day and R = .31 for I = 1 E/m^2 day. r^2 gives the fraction of the variance of R that is explained by the above model.

At depths of 10 m or more where the light is well diffused the minimum extinction is generally about 0.2 m^{-1}, due to absorption by the water itself and by dissolved organic pigments. Additional extinction is due to suspended particles (seston) in the water; these are mainly inert mineral particles in the range of sizes called silt (.004 to .062 mm), with a greater or less fraction of organic particles and phytoplankton. Careful measurements off San Onofre have shown fairly close linear relations between extinction and the cross section or simply the weight concentration of total seston in the water, independent of the organic content of the seston (the mineral particles are smaller but denser and more absorptive than the organic particles).

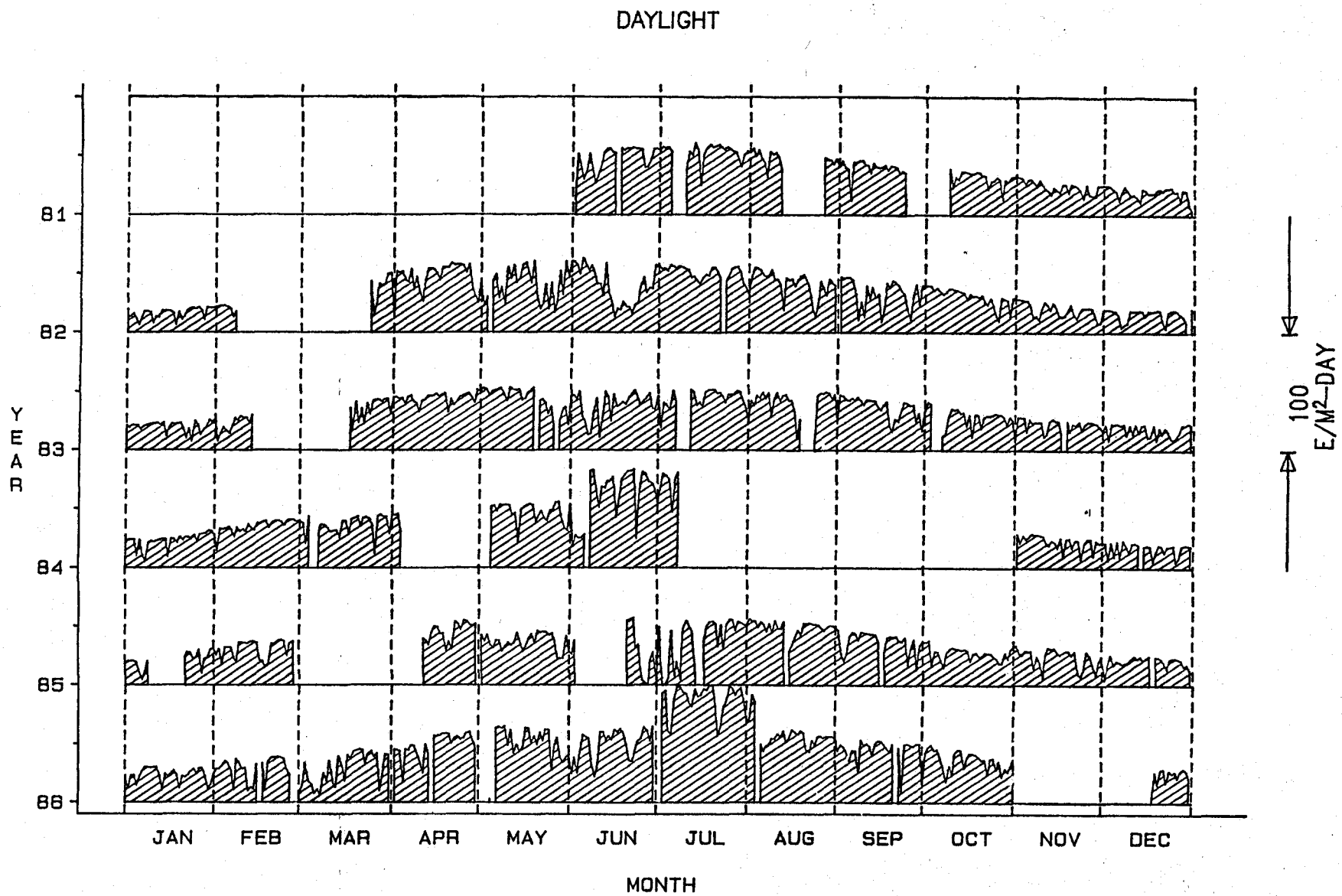

Figure 4-9. Daily daylight irradiance

The linear relation between daily extinction K (m^{-1}) and seston concentration S_w (mg/liter) is given by

$$K = .264 + .0016\ S_w$$

with r^2 = .51 (see Reitzal et al, 1987, Measurements of suspended particles utilizing pump system).

Most of the time, the immediate source of suspended mineral particles is the sediment on the bottom, which is intermittently resuspended by waves and swells. The ultimate sources of this sediment are the runoff of rivers and streams, and the erosion of the backshore and bluffs by storm waves. The water velocities at the sea bottom in the back-and-forth surges produced by waves are greater in shallower water; nearshore sediments are more often resuspended, as well as being closer to the original sources on shore, so the seston load and extinction are generally larger closer to shore. Since the seston continually settles downward in the water column, seston load and extinction also generally increase toward the bottom.

The original sources of seston are both seasonal and localized; the silt grains that predominate on the bottom several kilometers from shore probably require at least several or perhaps many episodes of resuspension by waves and transport and dispersal by currents to reach their equilibrium depth and distance from shore. The great variation among times and places in the way extinction responds to wave episodes indicates that finer-than-normal particles on the bottom in depths up to 14 m occur in transitory patches.

Figures 4-10 and 4-11 give time histories of daily irradiance at 14 m depth over the years 1981-1986 at two stations, SMK45 and SOK45 (see Section 3). These show the annual cycle of surface irradiance, with episodic changes due to variations in extinction. They also show the large overall increase in irradiance during the El Nino years, due to the large scale replacement of coastal water with oceanic surface water from several hundred kilometers offshore. Table 4-2 gives the statistics of daily bottom irradiance.

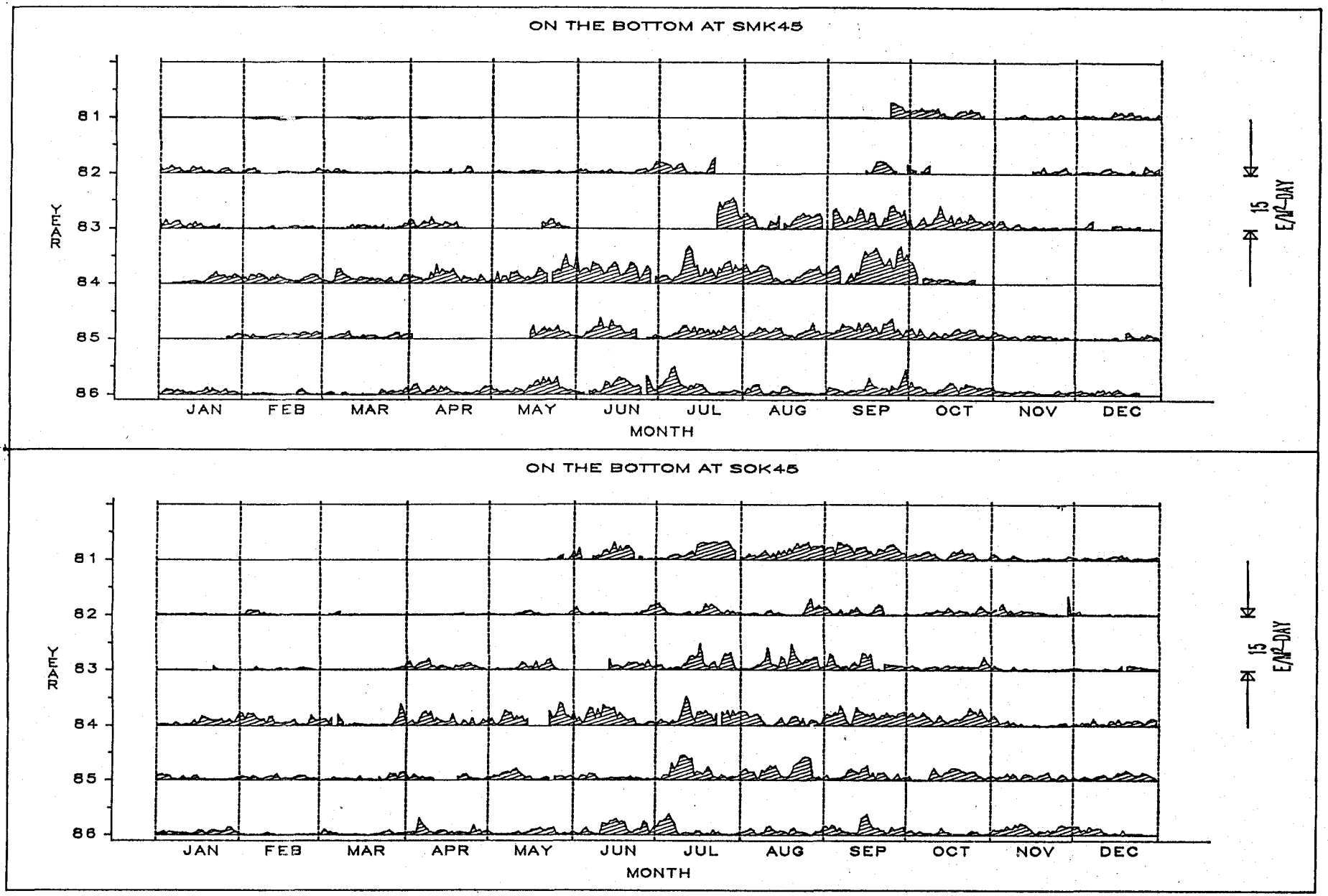

Figure 4-10. Time histories of daily irradiance 2 m above the bottom

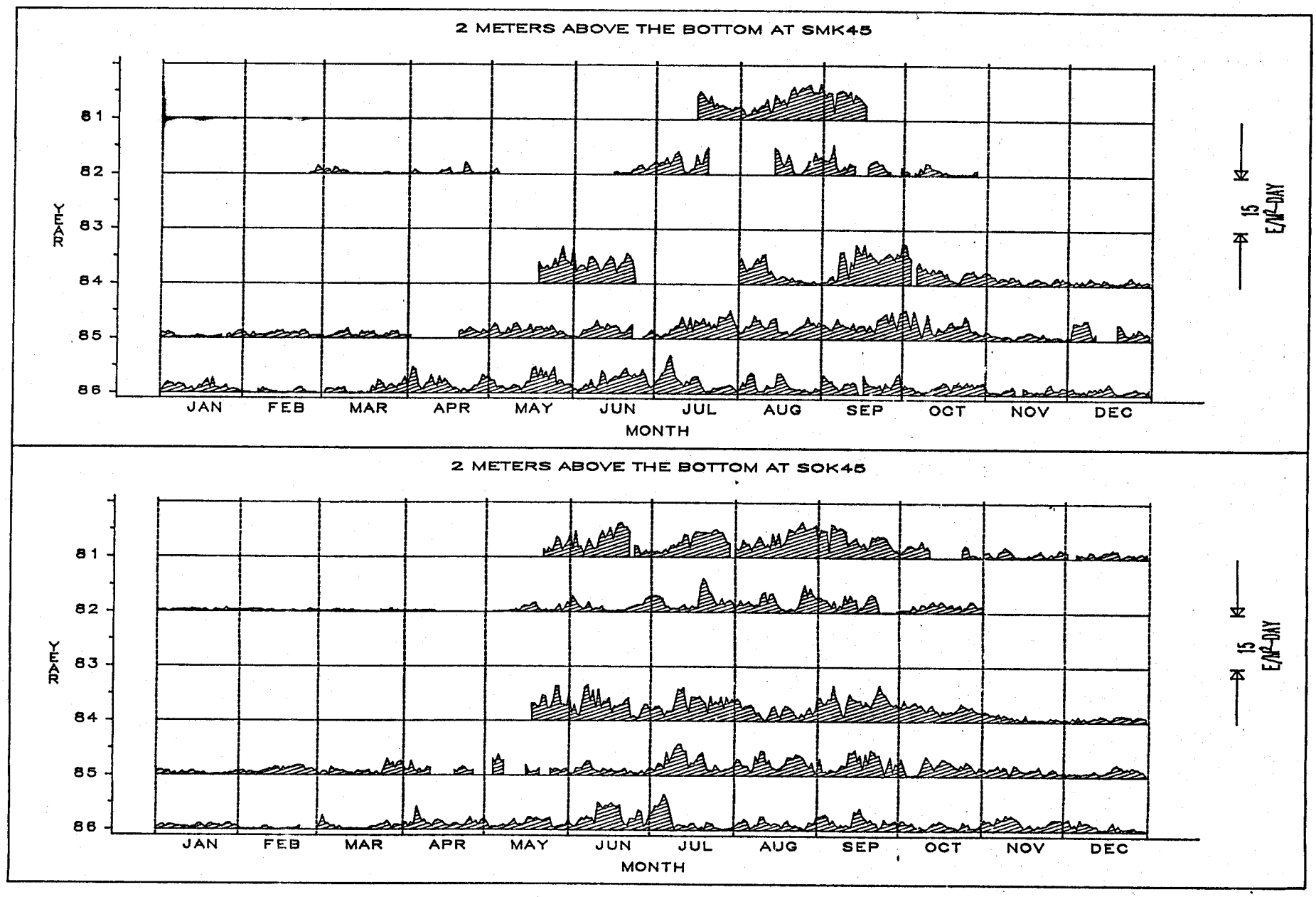

Figure 4-11. Time histories of daily irradiance on the bottom

TABLE 4-2

STATISTICS OF BOTTOM IRRADIANCE (E/M2-DAY)

		SMK45				SOk45			
YEAR	SEASON	MEAN	STD	MAX	N	MEAN	STD	MAX	N
81	SUMMER	0.5	1.2	4.1	43	2.2	1.5	5.0	130
81-82	WINTER	0.7	0.6	2.6	169	0.5	0.6	2.9	181
82	SUMMER	0.7	0.9	4.0	128	0.6	0.8	4.3	183
82-83	WINTER	0.5	0.5	2.3	144	0.4	0.6	5.1	176
83	SUMMER	2.5	1.9	8.2	99	1.6	1.4	7.2	164
83-84	WINTER	1.2	1.0	6.0	170	0.9	0.9	5.8	181
84	SUMMER	3.4	2.2	10.2	180	2.3	1.5	7.7	175
84-85	WINTER	1.0	0.9	6.1	89	1.0	1.0	4.9	182
85	SUMMER	2.2	1.2	5.6	138	1.5	1.6	7.4	174
85-86	WINTER	0.7	0.7	3.0	176	0.8	0.8	3.2	181
86	SUMMER	1.7	1.3	7.3	180	1.3	1.2	5.6	183
86-87	WINTER	1.1	0.7	2.8	81	1.0	0.8	3.1	92

4.3. Currents

Figure 4-12 shows daily averages of the longshore current composite time series plotted year by year, stacked above each other, for the entire data set from 1977 through 1986. This plot clearly shows the type of variability that the SONGS region experienced over the years on time scales from a few days to many months. Quantitative statistical analysis is done in the next section on this time series but many interesting features are readily seen from this presentation:

- Downcoast fluctuations occur more often than upcoast fluctuations in all the years.
- Upcoast currents persist typically for only a few days, occasionally lasting 10 days to 2 weeks while downcoast currents persist regularly for one to two weeks, sometimes lasting a month or more.
- Stronger more persistent downcoast currents occur in the summer months compared to the winter months.
- The years 1979 and 1985 show the mildest longshore current fluctuations on daily time scales, a fact that is even more apparent when examining variances.

4.3.1. Descriptive statistics

Tables 4-3a and 4-3b show the statistics of the longshore current (V) and the cross-shore current (U) from the composite time series for 3 meters below the water surface (MLLW) for total water depths between 10 and 15 meters. These tables give the mean (positive upcoast), standard deviation (STD), maximum values in the up and downcoast directions, skewness, kurtosis, and number of hourly data points, (N), for the individual summers (April - September) and winters (October - March) for all the summers and winters where data were available. Cummulative summer and winter statistics are also given.

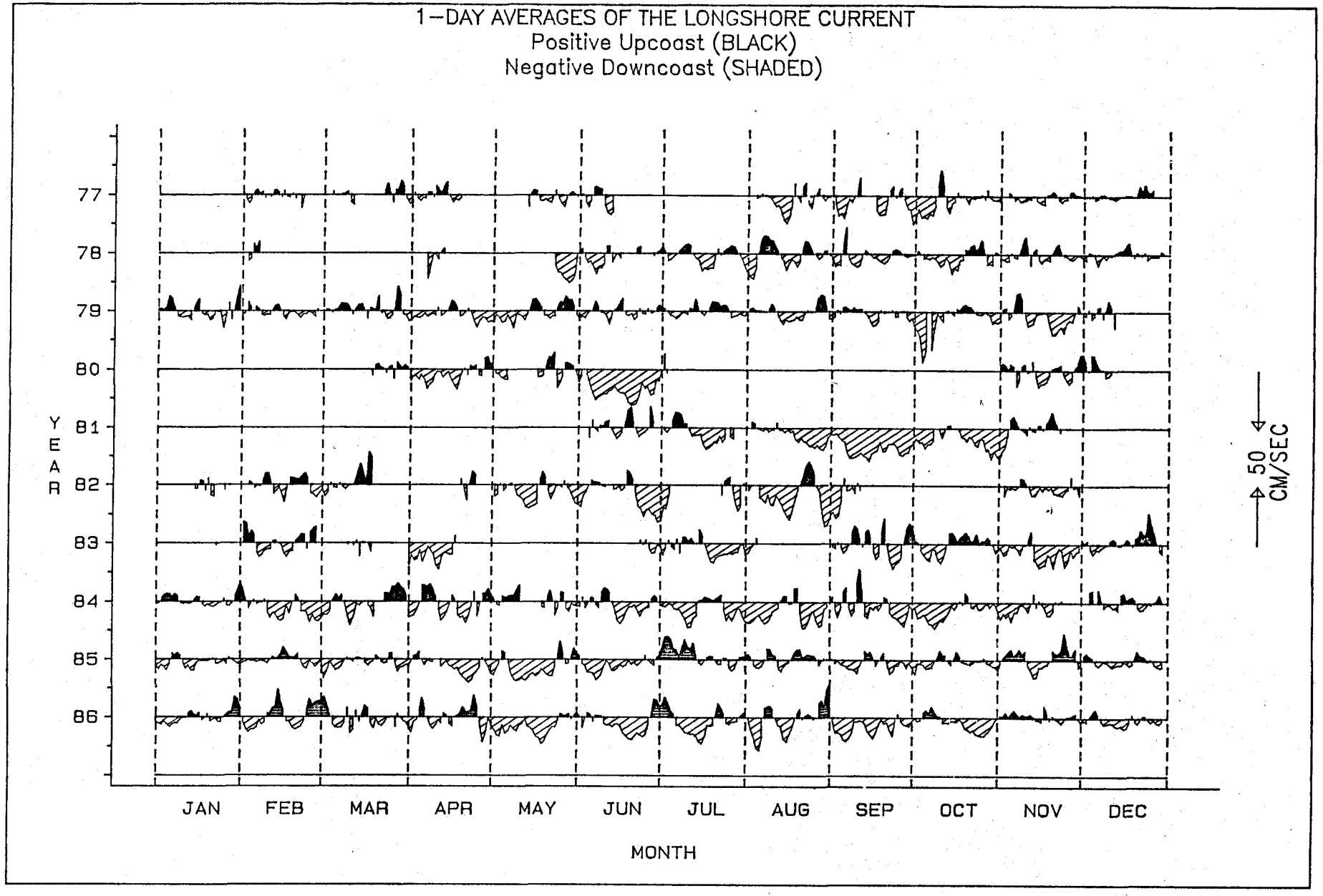

Figure 4-12. Ten-year history of daily mean longshore current. The portions shaded in black are the currents travelling up the coast (towards Los Angeles) and the hatched portions are the downcoast currents

TABLE 4-3a LONGSHORE CURRENT STATISTICS

YEAR	SEASON	MEAN	STD	UPCOAST MAX	DWNCOAST MAX	SKEWNESS	KURTOSIS	N
77	SUMMER	-3.4	9.5	28.6	39.0	-0.4	3.7	2525
77-78	WINTER	-1.7	8.1	27.9	35.6	-0.2	5.0	2120
78	SUMMER	-3.0	9.9	42.0	37.6	-0.3	3.8	3128
78-79	WINTER	-0.4	7.9	37.2	35.6	0.2	4.9	4345
79	SUMMER	-1.2	7.0	20.0	29.3	-0.1	3.3	4391
79-80	WINTER	-3.7	11.6	29.0	61.4	-1.1	5.7	2068
80	SUMMER	-8.2	12.8	30.4	46.4	-0.3	2.7	2006
81	SUMMER	-7.8	11.4	29.4	41.8	0.0	3.0	2614
81-82	WINTER	-2.7	10.9	34.6	41.3	-0.1	3.8	2488
82	SUMMER	-7.5	13.4	30.2	50.2	-0.2	2.8	2799
82-83	WINTER	-1.0	9.0	37.1	25.1	0.9	4.7	1595
83	SUMMER	-3.8	11.2	36.9	32.7	0.3	3.0	2136
83-84	WINTER	-1.9	10.4	41.0	46.0	-0.2	3.6	4293
84	SUMMER	-4.2	11.3	36.5	45.5	0.0	3.1	4223
84-85	WINTER	-3.2	7.8	20.2	40.8	-0.6	4.3	4092
85	SUMMER	-2.6	9.3	27.9	32.2	-0.2	3.2	4333
85-86	WINTER	-0.5	8.0	31.5	27.6	0.4	3.8	4345
86	SUMMER	-4.6	11.3	37.5	35.0	0.1	3.1	4392
86-87	WINTER	-1.9	6.9	20.3	26.9	-0.3	3.6	2185
ALL	SUMMER	-4.3	10.8	42.0	50.2	-0.3	3.4	32547
ALL	WINTER	-1.7	9.1	41.0	61.4	-0.3	4.9	28515
ALL	DATA	-3.1	10.1	42.0	61.4	-0.3	4.0	61062

TABLE 4-3b CROSS SHORE CURRENT STATISTICS

YEAR	SEASON	MEAN	STD	UPCOAST MAX	DWNCOAST MAX	SKEWNESS	KURTOSIS	N
77	SUMMER	0.7	4.1	13.4	15.0	-0.0	3.1	2525
77-78	WINTER	-0.4	4.1	12.4	15.8	-0.6	4.3	2120
78	SUMMER	0.3	3.7	16.1	15.4	-0.0	4.3	3128
78-79	WINTER	0.2	2.1	8.7	10.8	-0.2	4.5	4345
79	SUMMER	-0.6	2.2	7.6	10.3	-0.1	3.7	4391
79-80	WINTER	0.2	4.5	17.5	24.4	-0.6	6.2	2068
80	SUMMER	-3.0	5.7	16.8	24.5	0.1	3.3	2006
81	SUMMER	2.0	4.8	24.1	11.4	-0.0	2.7	2614
81-82	WINTER	-0.6	4.2	14.2	16.8	-0.4	3.9	2488
82	SUMMER	-0.7	4.9	17.2	20.0	0.1	3.6	2799
82-83	WINTER	0.6	3.4	17.2	18.6	-0.1	5.9	1595
83	SUMMER	1.3	6.2	24.0	22.2	0.4	3.9	2136
83-84	WINTER	-3.3	5.0	18.2	45.9	-0.8	6.8	4293
84	SUMMER	-3.4	6.7	24.9	28.9	0.0	2.9	4223
84-85	WINTER	-0.9	6.5	21.7	45.9	-1.2	9.2	4092
85	SUMMER	1.0	4.5	24.8	14.9	1.0	5.1	4333
85-86	WINTER	0.6	3.8	15.6	14.4	-0.4	4.2	4345
86	SUMMER	1.9	5.6	24.8	17.4	0.0	3.9	4392
86-87	WINTER	1.1	3.3	15.3	14.2	0.2	4.5	2185
ALL	WINTER	-0.4	4.5	21.7	45.9	-1.1	9.7	28515
ALL	SUMMER	-0.1	5.3	24.9	28.9	-0.0	4.4	32547
ALL	DATA	-0.2	5.0	24.9	45.9	-0.4	6.3	61062

Tables 4-4a and 4-4b give similar statistics for currents at various depths in the water column and three total water depths, < 10 meters, 10-15 meters, and > 20 meters. Measurements at the same water depth and depth from MWL are averaged together to construct a single representative time series. Also the seasons between 1978 and 1980 are averaged together in these statistics since this was the period in which the arrays extended adequately to the various depths. The standard deviations and maximum values all confirm that current fluctuations are stronger as one moves into deeper total water depths. Near surface currents are also more energetic than deeper currents in any given total water depth.

Table 4-5 gives additional statistics for the longshore composite time series (hourly values, measurements at 3 m below mean water level) showing the mean of the downcoast currents, the mean of the upcoast currents, and the percentage of time that downcoast and upcoast hourly averages were observed. This is of particular value in assessing the likely exposure to discharged waters. It shows that downcoast currents can dominate up to 75% of the time during summer, and never below 54%.

Figures 4-13 and 4-14 show histograms of U and V for individual seasons. These plots show at a glance the spread in velocity fluctuations over the seasons and over the years. One sees that both summer cross shore and longshore currents are spread over a larger velocity distribution than their winter counterparts. This may be explained by energetic internal waves present in summer and considerably weaker in winter. Another noteworthy feature is seen in the summer longshore currents. The years 1979 and 1985 are appreciably different from the other years indicating these were unusually mild years with respect to longshore current fluctuations.

Figures 4-15 through 4-17 show more detailed histograms and cummulative distribution diagrams for all data, summer and winter.

TABLE 4-4a

LONGSHORE CURRENT STATISTICS FOR VARIOUS WATER DEPTHS

SEASON	WATER DEPTH	SENSOR DEPTH	MEAN	STD	UPCOAST MAX	DWNCOAS MAX	SKEWNESS	KURTOSIS	N
WINTER	<10	3	-0.5	7.3	31.0	35.3	0.1	5.0	4410
SUMMER	<10	3	-0.8	7.9	33.7	38.3	-0.7	5.4	6722
WINTER	10-15	3	-1.1	10.7	39.5	61.4	-0.5	5.8	7361
SUMMER	10-15	3	-4.4	11.2	55.8	52.2	-0.5	4.1	8365
WINTER	>20	3	-3.1	15.2	56.8	65.9	0.2	3.7	9476
SUMMER	>20	3	-6.8	15.6	45.2	52.4	-0.1	2.6	9706
WINTER	10-15	9	0.1	7.3	37.0	31.2	0.3	4.2	9276
SUMMER	10-15	9	0.6	6.7	46.9	28.7	0.3	6.2	8253
WINTER	>20	9	-1.1	12.0	40.3	55.9	-0.3	4.2	8117
SUMMER	>20	9	-5.8	14.1	55.5	48.0	-0.1	2.5	8383
WINTER	>20	21	0.5	12.5	68.2	51.0	-0.1	5.8	10716
SUMMER	>20	21	-0.9	10.3	33.6	34.9	-0.3	2.9	11394

TABLE 4-4b

CROSS SHORE CURRENT STATISTICS FOR VARIOUS WATER DEPTHS

SEASON	WATER DEPTH	SENSOR DEPTH	MEAN	STD	ONSHORE MAX	OFFSHORE MAX	SKEWNESS	KURTOSIS	N
WINTER	<10	3	0.3	2.7	13.2	13.2	-0.4	5.0	4410
SUMMER	<10	3	-0.3	3.3	16.8	21.8	0.2	6.7	6722
WINTER	10-15	3	0.1	3.3	17.5	24.4	-0.5	7.1	7361
SUMMER	10-15	3	-1.1	4.7	16.1	24.5	-0.5	4.1	8365
WINTER	>20	3	-1.0	6.9	28.5	28.3	-0.2	3.9	9476
SUMMER	>20	3	-1.8	8.3	36.8	44.2	-0.7	5.6	9706
WINTER	10-15	9	0.6	3.0	18.2	19.8	-0.4	7.0	9276
SUMMER	10-15	9	0.6	4.0	21.2	15.6	0.2	4.2	8253
WINTER	>20	9	0.1	6.2	31.8	33.5	0.0	4.4	8117
SUMMER	>20	9	-0.7	6.7	26.3	45.1	-1 0	6.0	8383
WINTER	>20	21	0.1	5.7	30.3	34.6	-0.6	5.9	10716
SUMMER	>20	21	0.1	4.5	19.0	29.4	-0.7	5.8	11394

TABLE 4-5 ADDITIONAL LONGSHORE CURRENT STATISTICS
3 Meters Below Water Surface

YEAR	SEASON	MEAN DOWNCOAST	MEAN UPCOAST	PERCENT DOWNCOAST	PERCENT UPCOAST
77	SUMMER	9.0	5.4	61.1	38.9
77-78	WINTER	6.2	4.9	59.9	40.1
78	SUMMER	9.2	5.7	58.7	41.3
78-79	WINTER	5.8	6.0	54.3	45.7
79	SUMMER	5.7	5.3	59.1	40.9
79-80	WINTER	10.6	5.9	58.0	42.0
80	SUMMER	13.8	6.6	72.9	27.1
81	SUMMER	12.5	6.1	74.7	25.3
81-82	WINTER	9.1	7.3	61.0	39.0
82	SUMMER	13.8	7.4	70.4	29.6
82-83	WINTER	6.4	8.0	62.6	37.4
83	SUMMER	10.0	8.8	66.8	33.2
83-84	WINTER	9.0	7.0	55.4	44.6
84	SUMMER	10.9	7.2	62.8	37.2
84-85	WINTER	7.2	4.6	66.4	33.6
85	SUMMER	8.3	5.9	59.7	40.3
85-86	WINTER	5.9	6.3	55.7	44.3
86	SUMMER	10.9	7.0	64.7	35.3
86-87	WINTER	6.2	4.3	58.9	41.1
ALL	WINTER	7.3	6.1	58.4	41.6
ALL	SUMMER	10.2	6.4	64.1	35.9
ALL	DATA	8.9	6.3	61.4	38.6

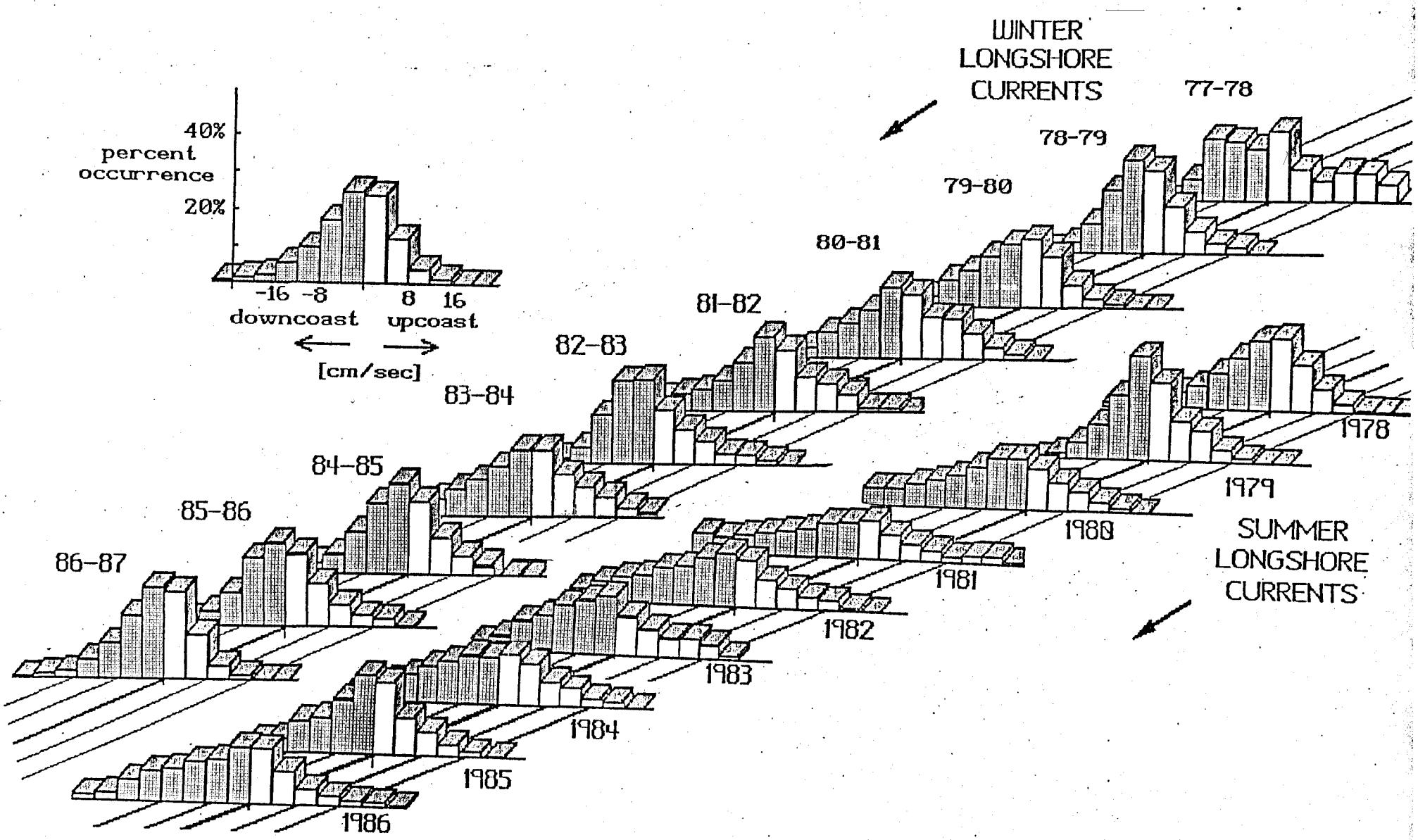

Figure 4-13. Histogram of the longshore current hourly-averaged values, season by season for 1977-1986

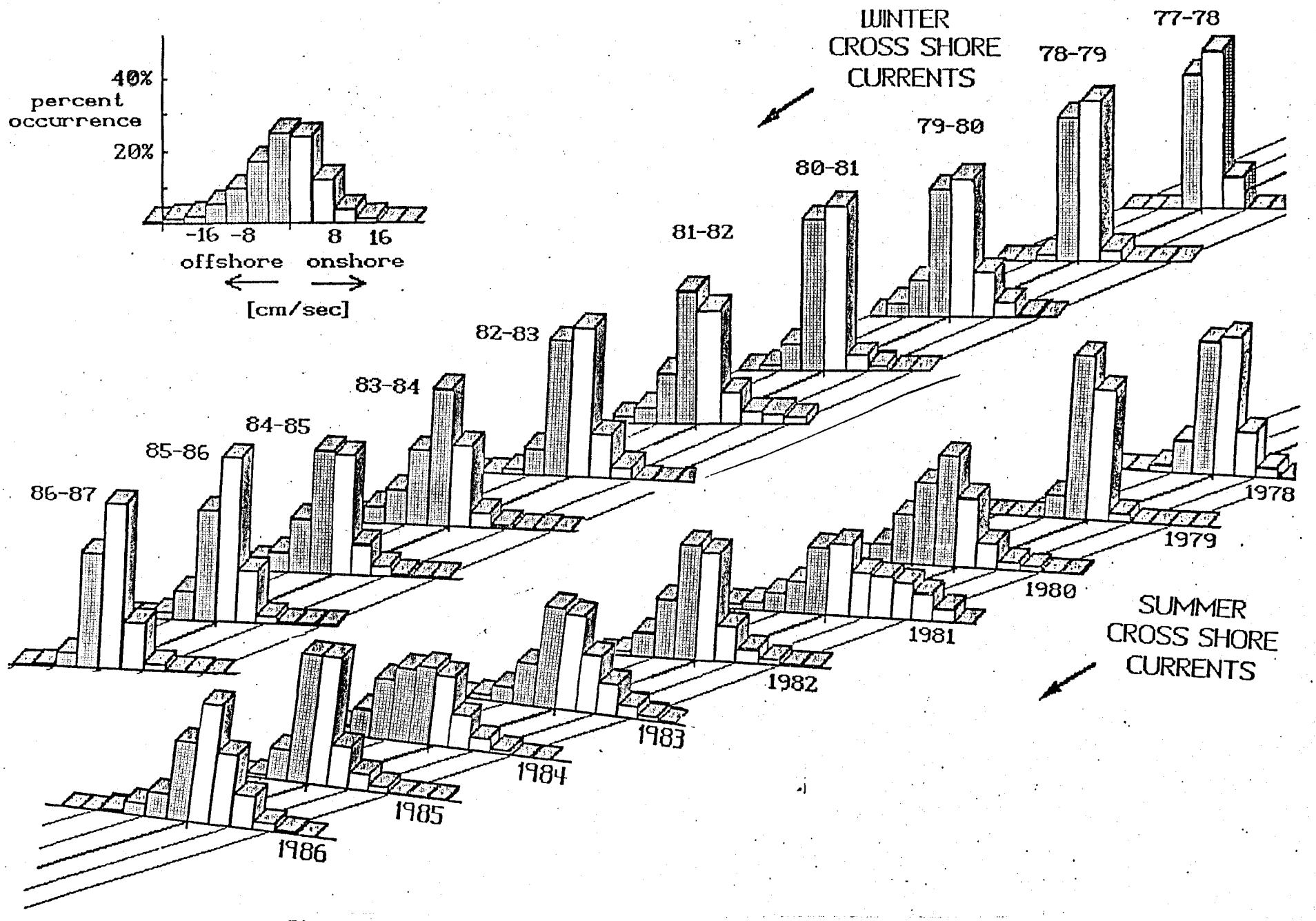

Figure 4-14. Histogram of the cross-shore current hourly-averaged values, season by season for 1977-1986

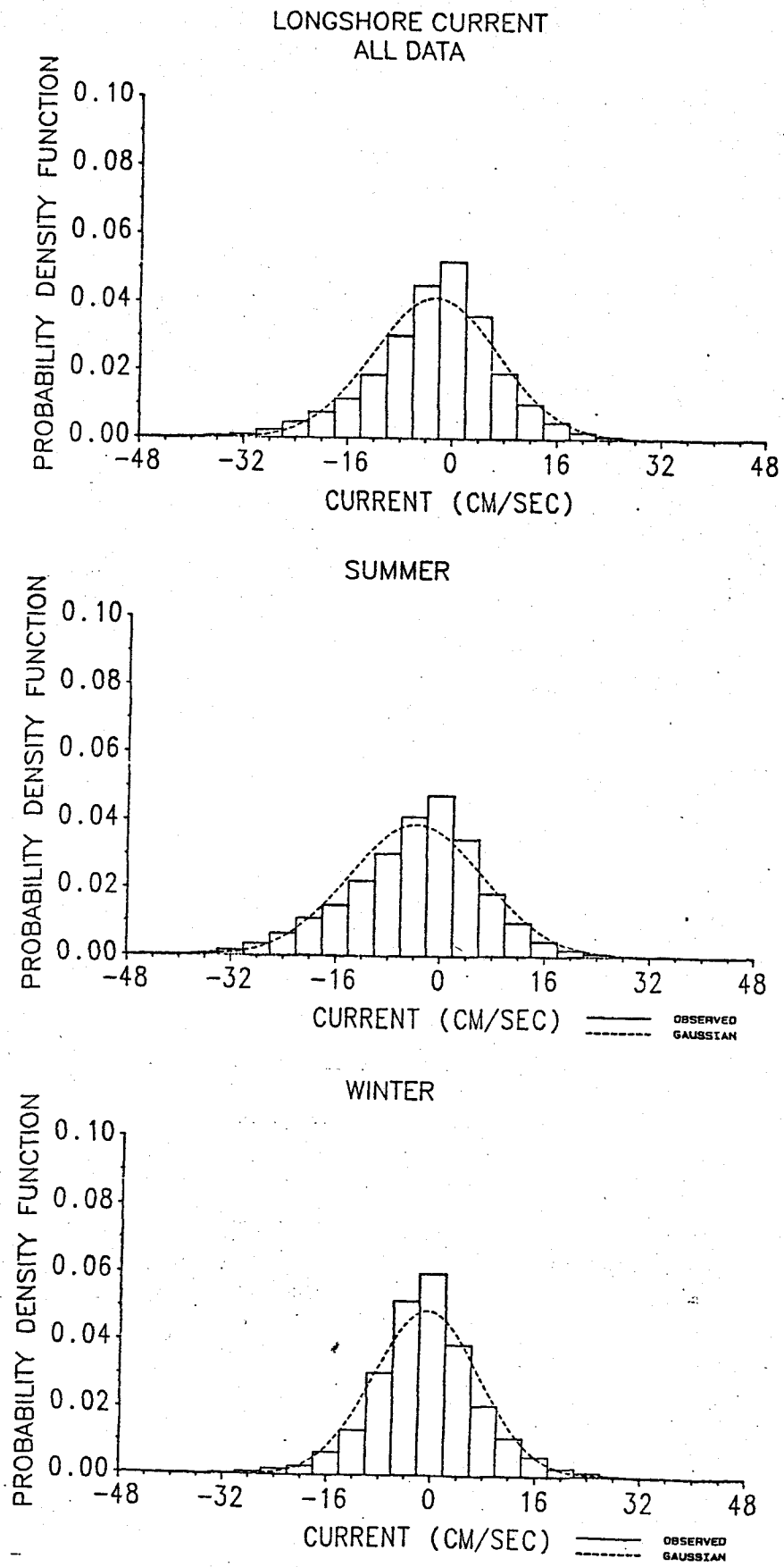

Figure 4-15. Comparison between the observed density distribution for longshore current and Gaussian distribution, for all data, summer and winter

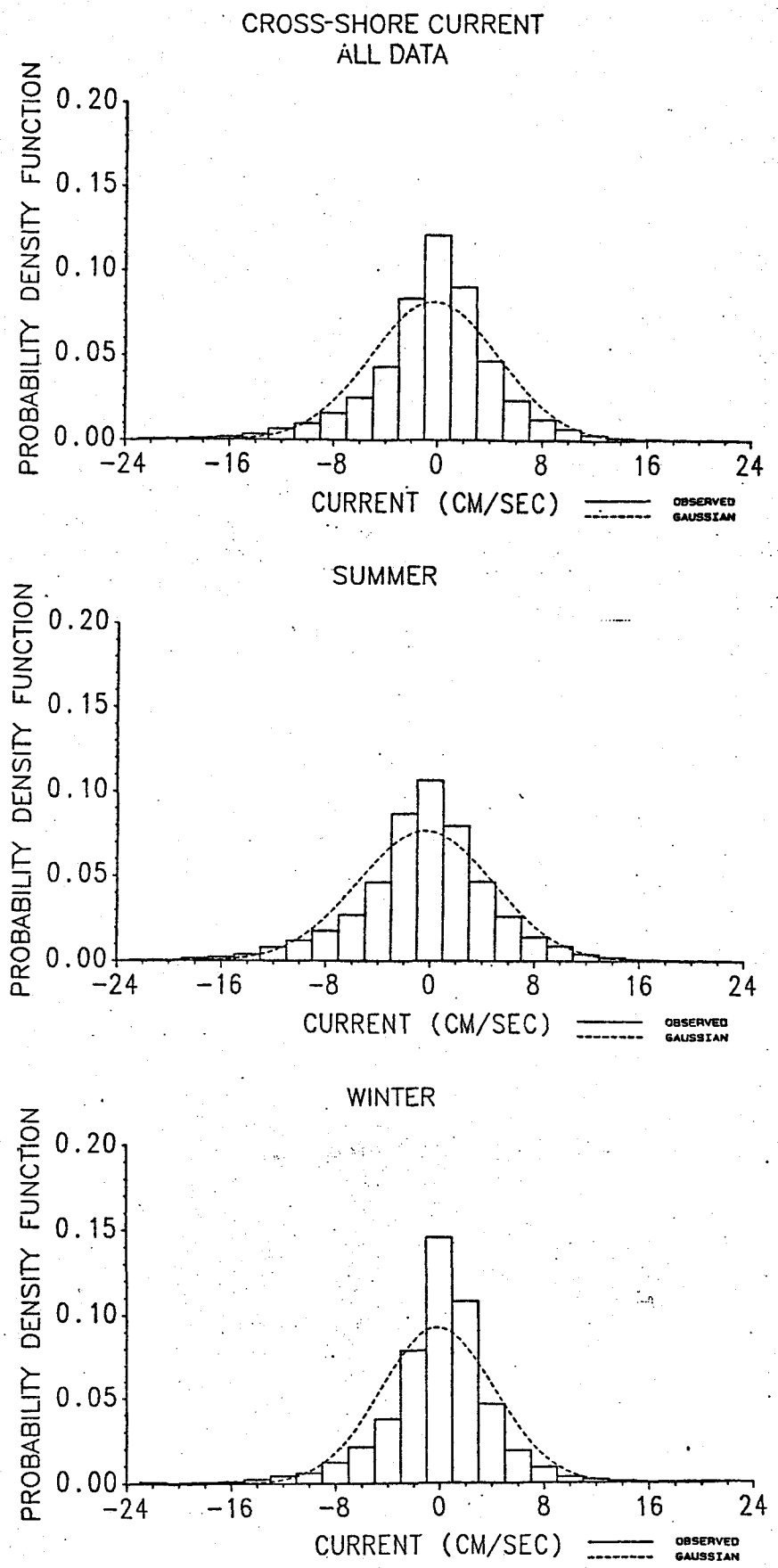

Figure 4-16. Comparison between the observed density distribution for cross-shore current and Gaussian distribution, for all data, summer and winter

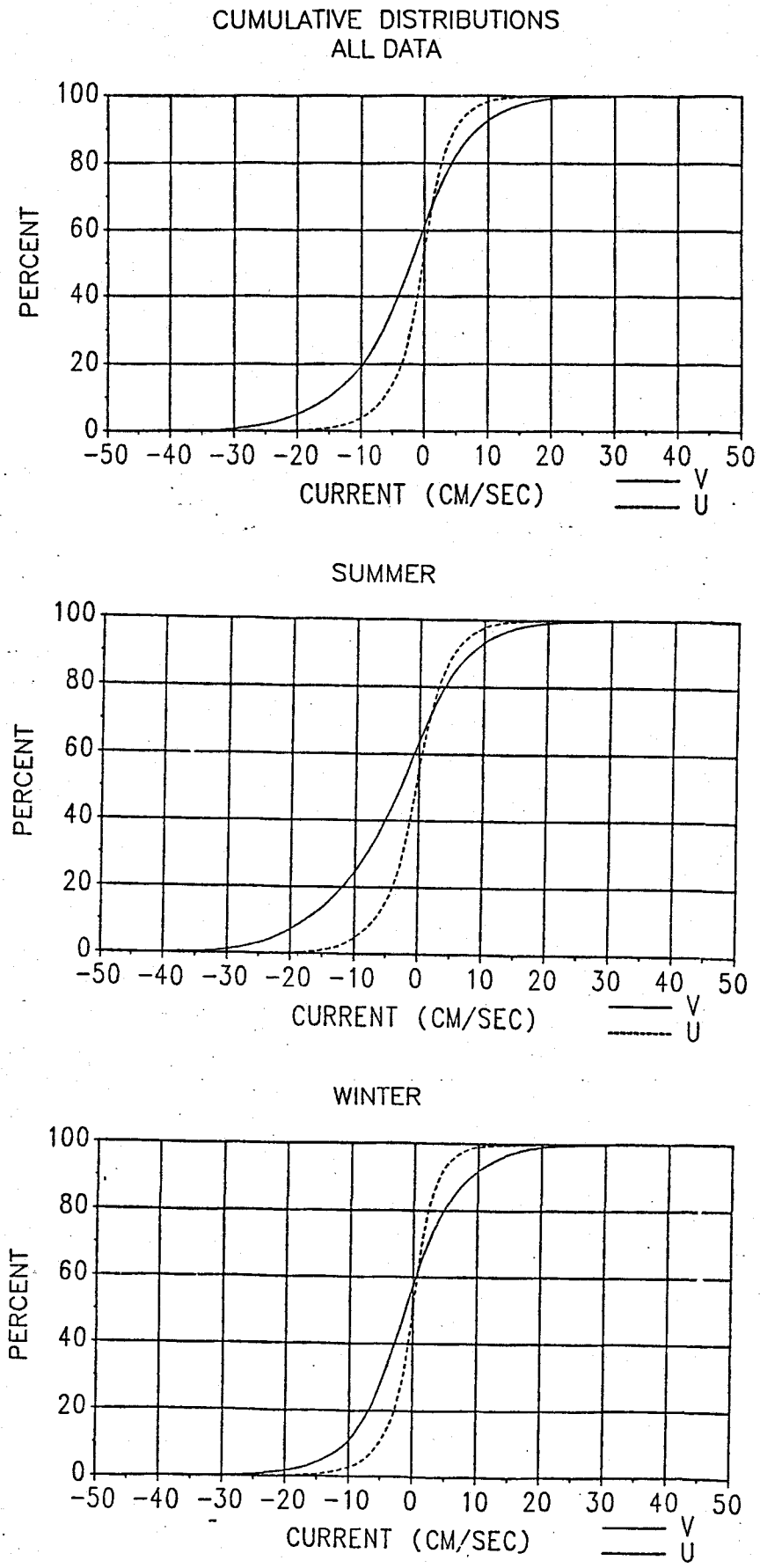

Figure 4-17. Cumulative distribution for longshore and cross-shore currents, for all data, summer and winter

Correlation matrices of V and U for all years are given in the Data Summary, Vol. VI-3 (Reitzel et al, 1987). We note that correlation coefficients of V are clearly larger in general than those of U, and increase with the total depth of water.

4.3.2. Spectra of the composite time series

Figure 4-18 presents one-sided spectra of the cross and longshore current components computed from the composite time series for the period from January 1, 1984 through December 31, 1986. Hourly averaged values of the currents were used and each spectral estimate has 32 degrees of freedom. The spectra of U and V contain notable peaks at 1, 2, 3, 4, and 5 cpd (cycles per day) corresponding to the diurnal tide, semi-diurnal tide, and the higher harmonics of the tidal motions. The longshore component contains more variance at low frequencies than the cross-shore component, indicating a polarization of the flow in the alongshore direction. The tidal components at 1 and 2 cpd also show this preference for the alongshore direction, although not quite as strongly. In the frequency range from 1 to 10 cpd, the cross-shore and longshore energies are similar. At the low frequency end (< .5 cpd), we see the characteristic red spectrum; the slope of the line through the spectral estimates decrease as $1/f^2$. There is some indication of a leveling off in the spectrum of the longshore components at frequencies whose periods are greater than 30 days. Very few time series taken anywhere in nearshore regions have been able to resolve these low frequency features before now.

Another interesting feature is the relative flat spot in the spectra occurring between .3 and .7 cpd. The dynamical interpretation of this may be that local wind events and storms lasting on the order of a few days do not input significant energy directly into these frequency bands. In other words, local, synoptic scale forcing in this area does not account for much of the observed variance. This has been noted by Lentz (1985, 1984) in Southern California shelf circulation studies.

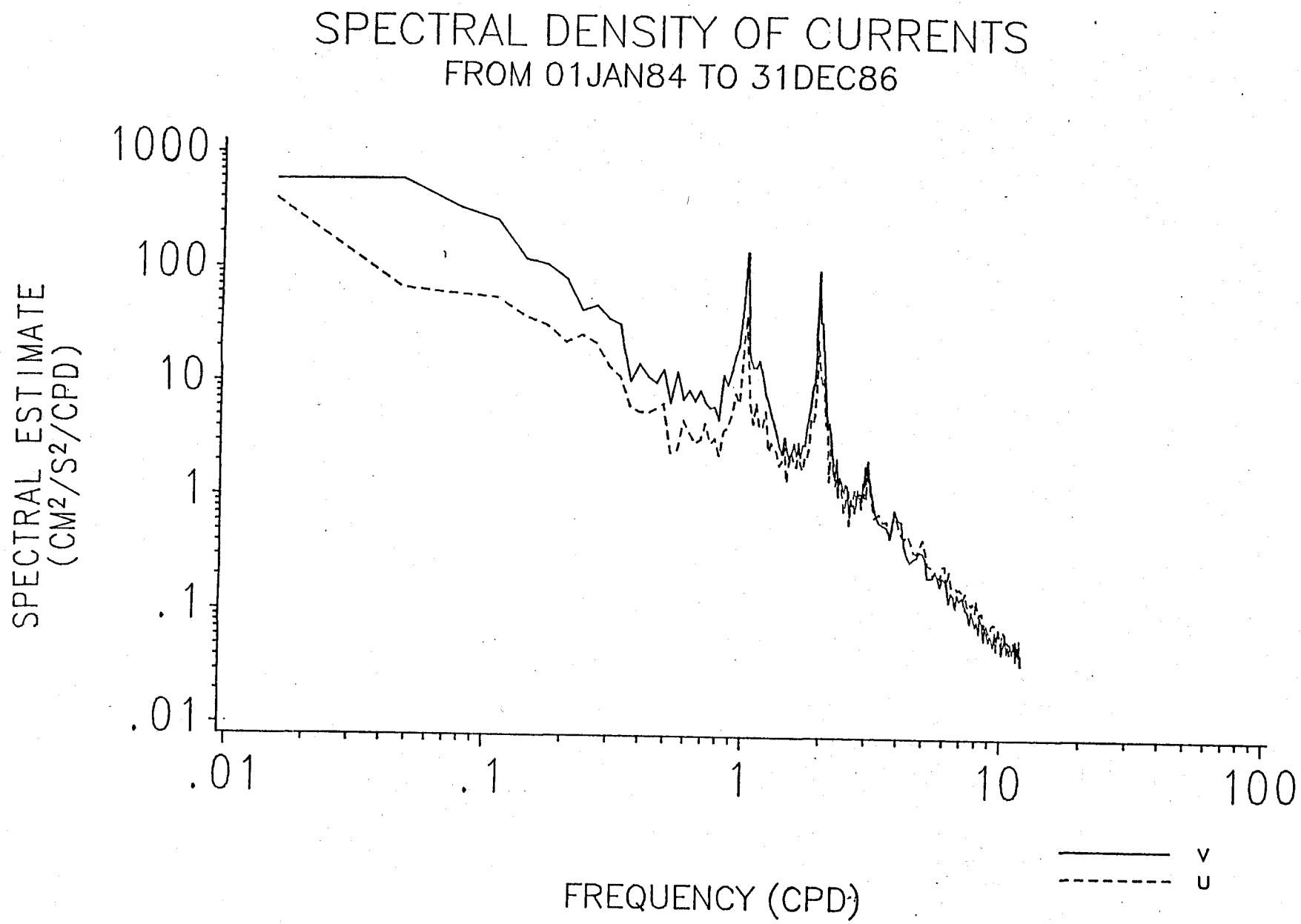

Figure 4-18. One-sided spectra for the cross-shore and longshore current components, from the composite time series for the period from Jan 1 1984 through Dec 31 1986

Figure 4-19 shows a collection of spectra for U and V for the individual seasons from 1984 through 1986. There are significant differences from season to season in the heights and widths of the tidal peaks at 1 and 2 cpd. This appears to be a reflection of how well tidal forcing couples with the local circulation. One such coupling is through internal waves that are supported in the water column when there is sufficient stratification. One can see in these spectra that the energies at 1 and 2 cpd for both U and V are higher in summer than their counterparts in winter. Also visible in these plots are the summer/winter differences in energy at the harmonics of the tides. Especially large is the energy at 3 cpd during summer relative to winter. These harmonics, believed to be generated by nonlinear interactions of the internal tides, have also been observed by Winant (1981).

An average spectra of U and V for the summer and winter seasons is presented in Figure 4-20. In order to examine how the energy of the current fluctuations is spread out amoung various frequency bands and to quantitatively compare summer and winter, we divide our frequency range into four bands: low frequency (< .8 cpd), a diurnal band (.8 - 1.6 cpd), a semi-diurnal band (1.6 - 2.4 cpd), and a high frequency band (> 2.4 cpd). Table 4-6 gives a summary of the variance estimates in the four frequency bands for the longshore and cross shore current components.

4.3.3. Persistence of longshore current

Duration is defined here as the number of successive hours over which the hourly mean velocity of current remains within a specified range. Two kinds of distributions are of interest for different purposes. One kind is simply a plot of how many duration events n(k) of length k occurred per year of record. Plots of this kind are shown in Figure 4-21 for the velocity ranges $|V| < 3$ cm/sec, $|V| < 6$ cm/sec, $|V| < 0$, and $|V| > 0$.

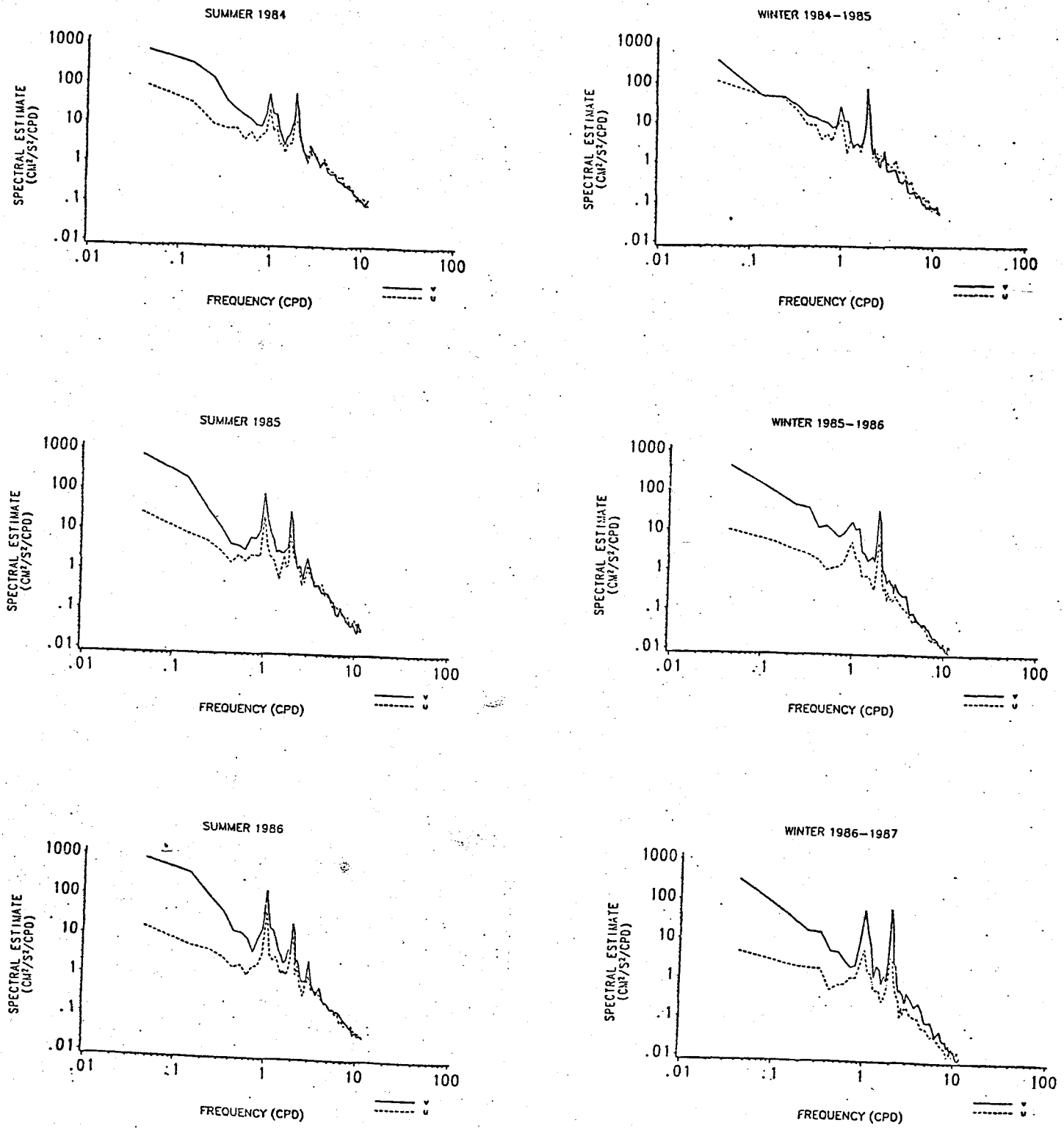

Figure 4-19. One-sided spectra of U (cross-shore) and V (longshore) current components by season from the period 1984-86

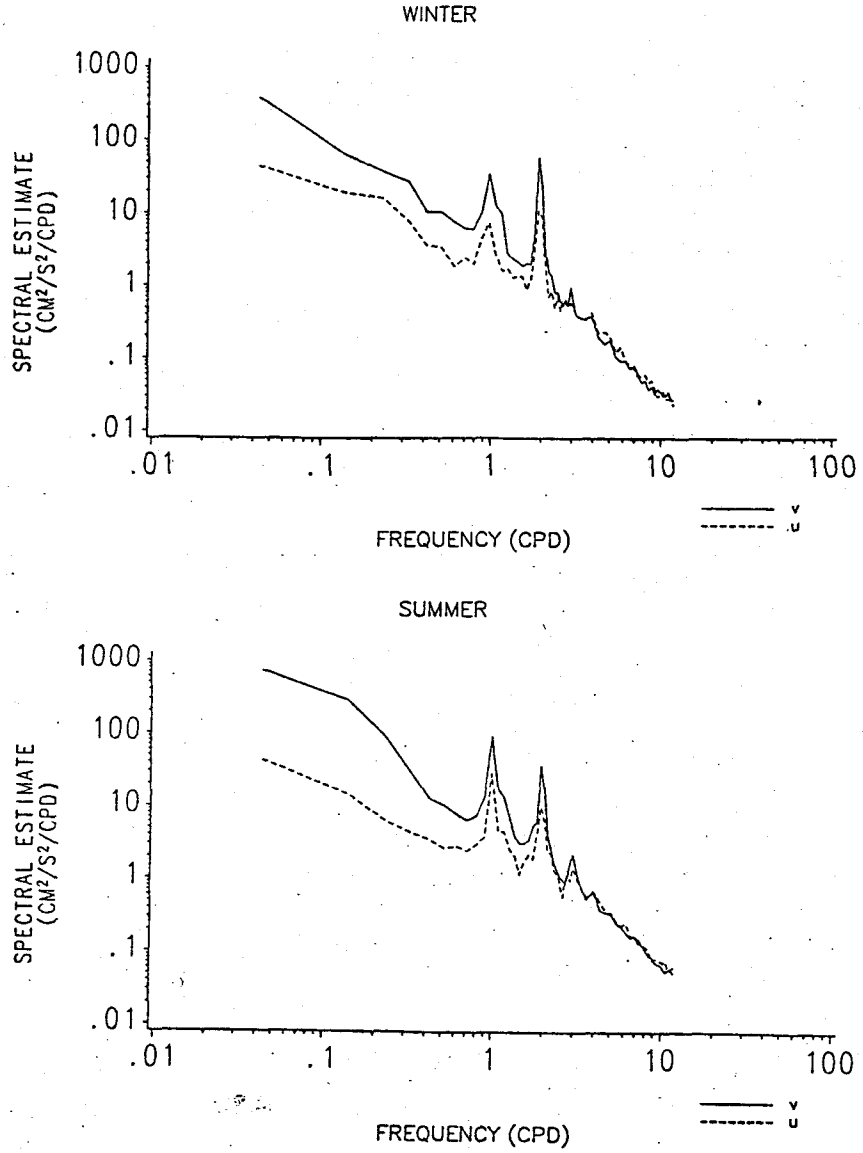

Figure 4-20. One-sided spectra for U (cross-shore) and V (longshore) current components formed by averaging the spectral estimates of the individual seasons between 1984-86

(see Figure 4-19)

TABLE 4-6

VARIANCE ESTIMATE FOR HOURLY LONGSHORE AND CROSS-SHORE CURRENT

SEASON	LONGSHORE CURRENT FREQUENCY BAND				CROSS SHORE CURRENT FRENCY BAND			
	Low <0.8 cpd	Diurnal 0.8-1.6 cpd	Semi-Diurnal 1.6-2.4 cpd	High >2.4 cpd	Low <0.8 cpd	Diurnal. 0.8-1.6 cpd	Semi-Diurnal 1.6-2.4 cpd	High >2.4 cpd
SUMMER	111.8	15.0	7.2	2.8	7.8	4.7	3.3	2.5
WINTER	50.7	7.3	9.2	1.5	9.4	2.2	2.9	1.4

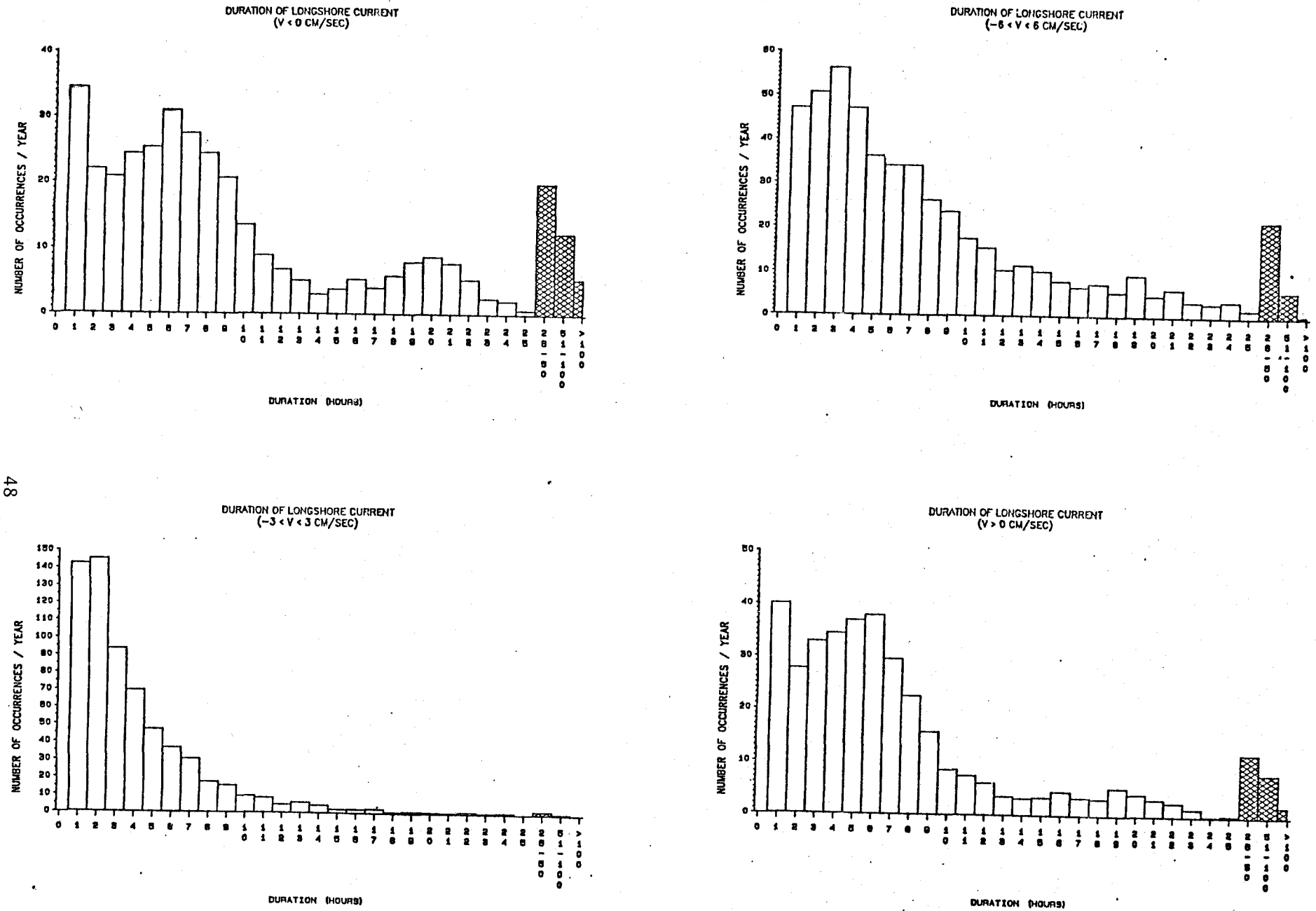

Figure 4-21. Number of occurrence per year of longshore current durations. Four ranges of current velocities are specified.

They show, for example, that slack water $|V| < 3$ lasting for 12 hours or more may be expected 10 times a year on the average, or that upcoast currents $|V| > 0$ lasting more than 3 days may be 5 times a year, while downcoast currents, lasting over 3 days may be expected 12 times a year.

The other kind of distribution is the fraction of all the hours having velocities within the range, which is involved in duration-events of length k ; that is,

$$f(k) = kn(k) \,/\, \sum_{k=1}^{\infty} kn(k).$$

The cumulative distribution of the above density distribution is shown in Figure 4-22. The results presented in this figure can be used in conjunction with the cumulative distribution of V (Figure 4-16) to estimate the percentage of time longshore currents flow between two velocity limits (upper and lower limits) with associated duration (duration range).

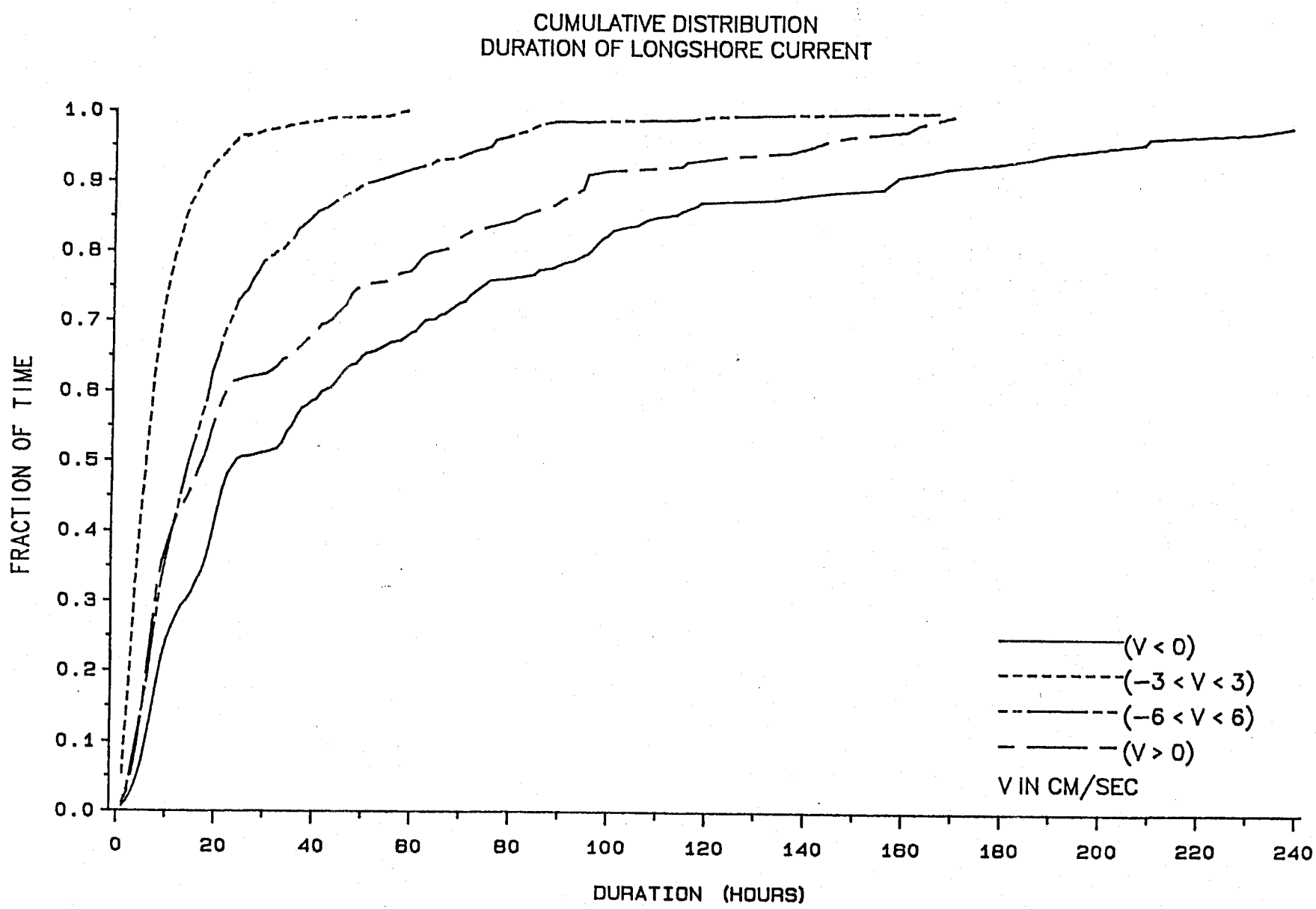

Figure 4-22. Cumulative distribution of longshore current duration for various current ranges

4.4 Waves

This section presents wave statistics for significant wave heights from a wave climate station located 1.8 km off SONGS, in 12 m of water. The recorded wave induced pressure at the level of the sensor is used to estimate the significant wave height. Descriptions of the instruments and the analysis techniques adopted for this study are given by Reitzel et al (1987, Vol. IV, Section 4.3.2).

Figure 4-23 shows daily average significant wave height, plotted year by year, for the entire data set from 1977 through 1986. This figure shows that the differences between individual years are larger than the usual differences between seasons; waves higher than 3 meters were not recorded except during the winter 1982-83, when they occurred six percent of the time; waves lower than .75 m were rare before 1985, but were frequent or even predominant the entire season of 1985-86. The period between May and December, 1986, was associated with calm wave conditions.

Figures 4-24 and 4-25 give the frequency and the cumulative distribution for the daily average significant wave height for all data, summer and winter seasons. In these figures, we indicated the mean, standard deviation (STD), root mean square (H_{rms}) of significant wave height over the years 1981-1986, and the number of daily data points (N). Notice that the difference between the means of significant wave height in winter and summer seasons are small. The seasons may be equalized by the greater frequency of swells from southerly directions in the summer and the occurrence of very high and frequent waves in winter. This is in agreement with values of standard deviation for summer and winter seasons.

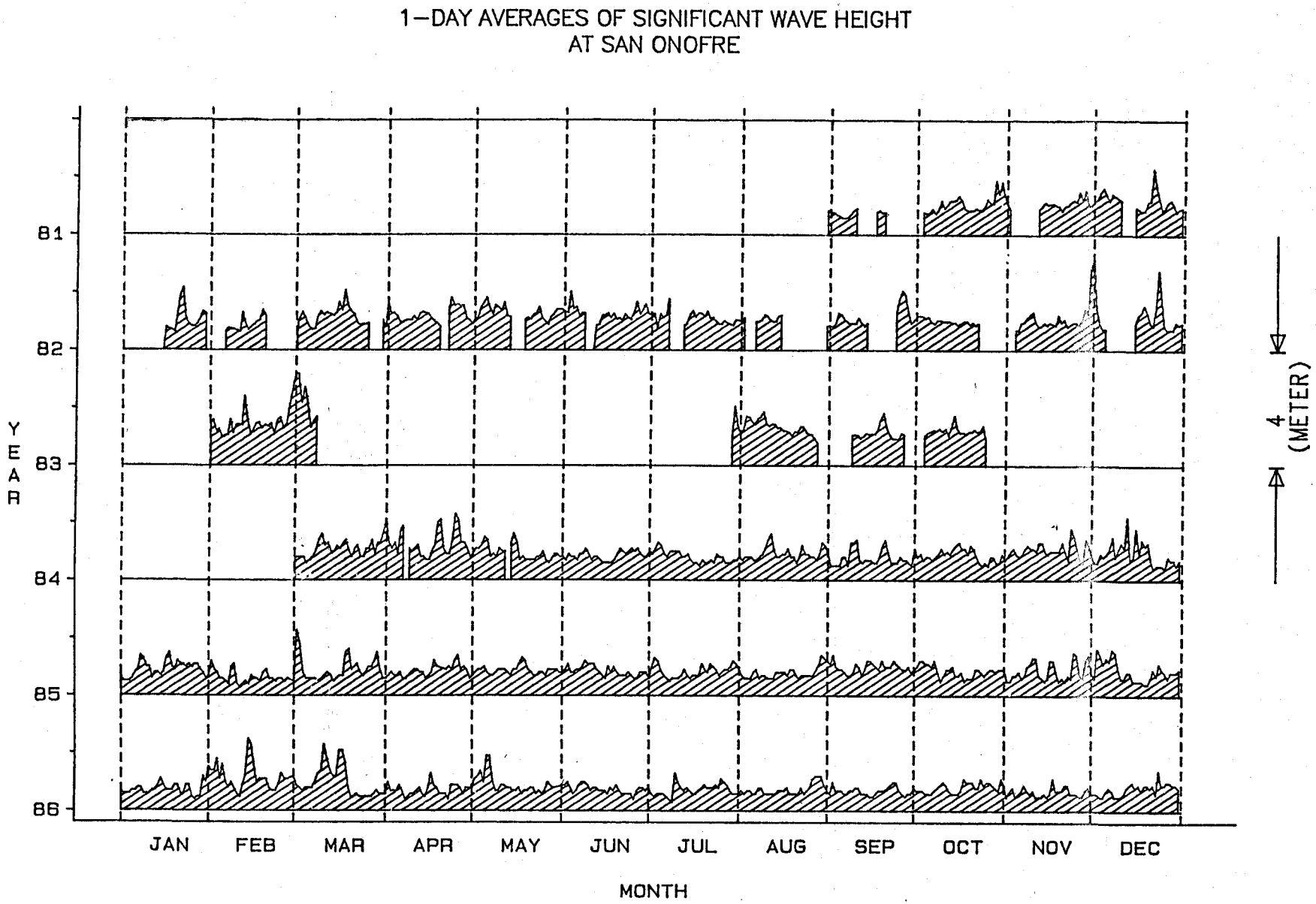

Figure 4-23. Time histories for significant wave height at San Onofre

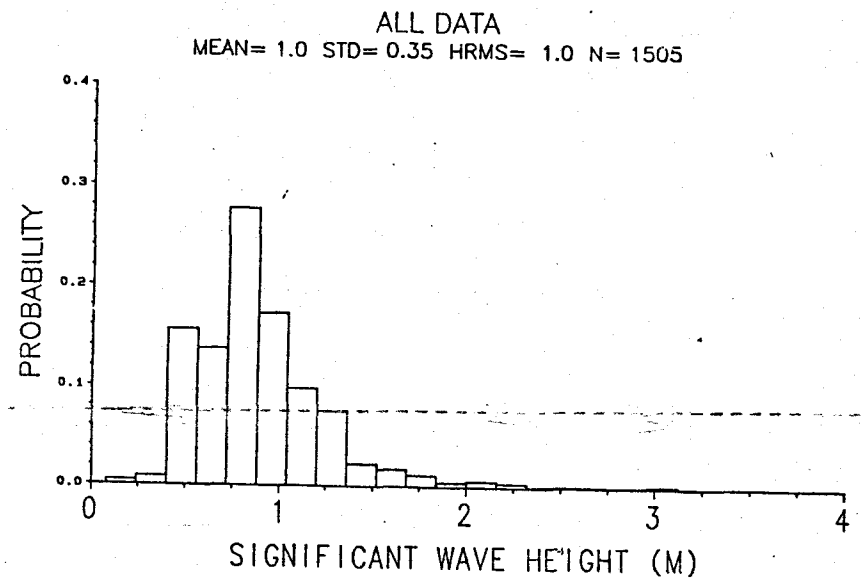

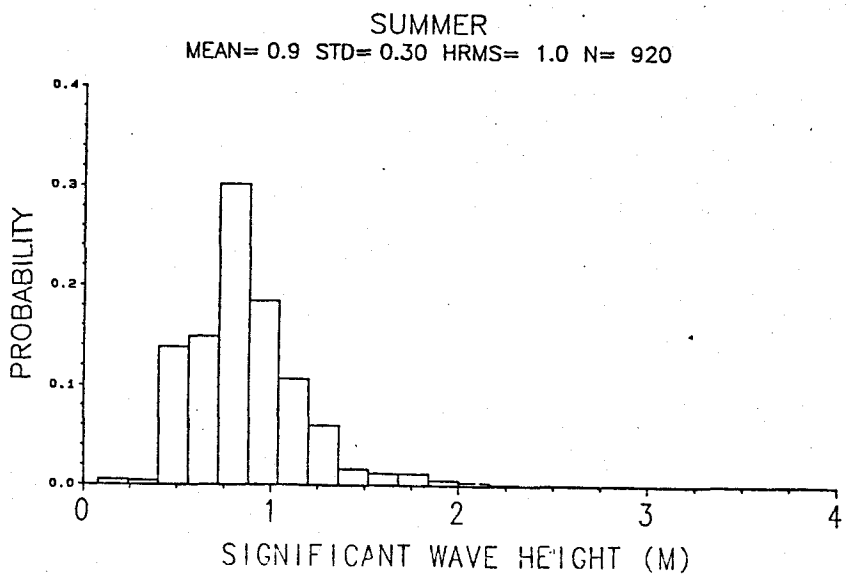

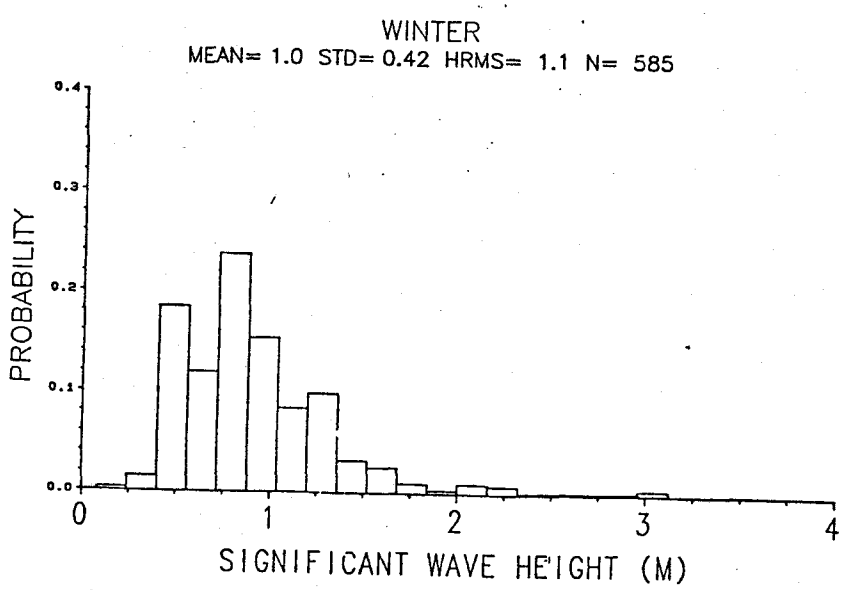

Figure 4-24. Histograms for significant wave height

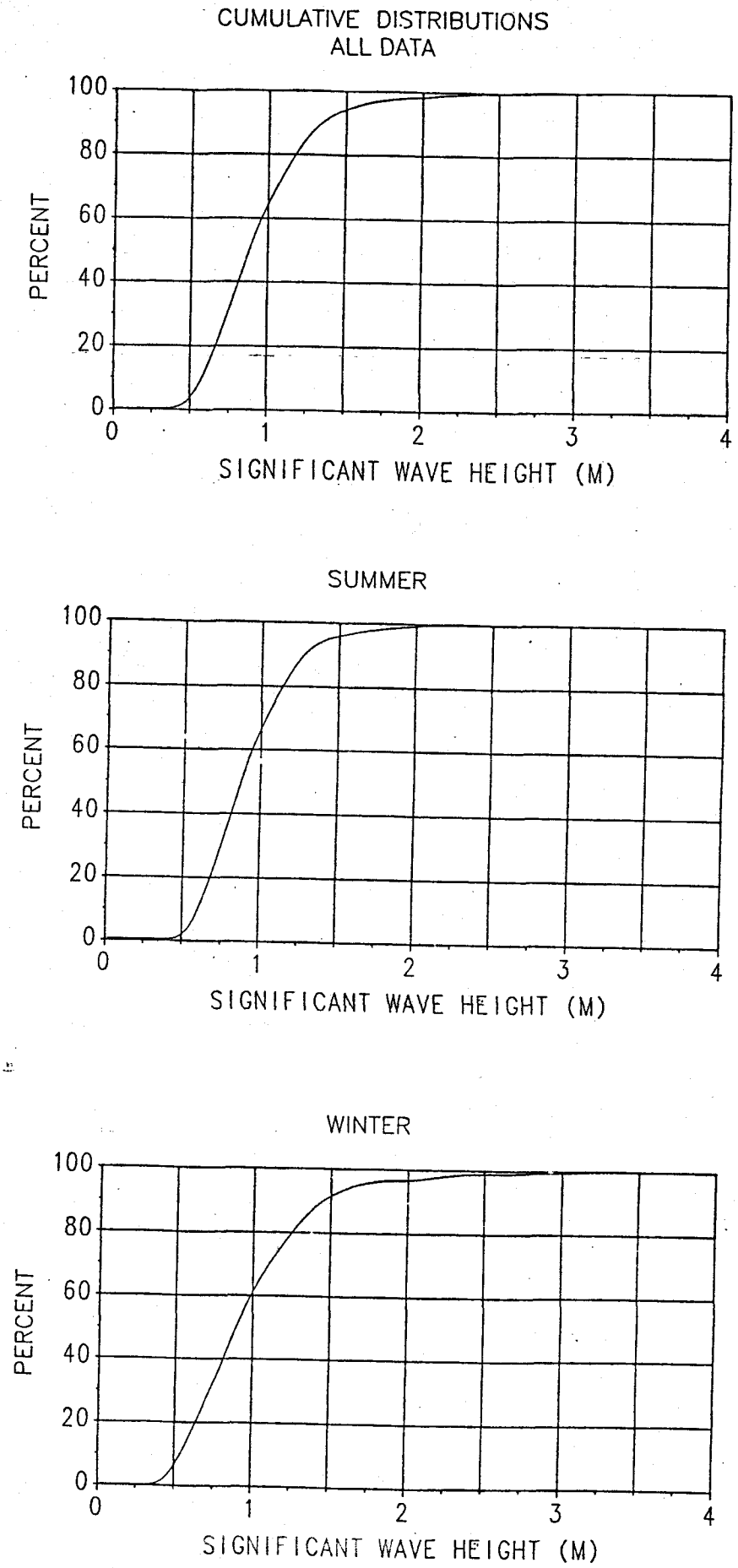

Figure 4-25. Cumulative distributions for significant wave height

4.5 Winds

Southern California (latitude 32° to 35° N) lies in the northern part of the doldrum belt between the westerly winds to the north and the northeast trade-winds to the south; its most persistent feature is a strong high pressure center frequently at about 35° N 140° W featuring sinking air and arid climate. During normal years, the whole wind system shifts southward with the thermal equator in winter, bringing winter storms with westerly wind, rain and waves. Unusual events, such as the El Nino event of 1982-83, are probably extreme southward shifts of the same kind, due to declines in the strength of the high pressure center and the northeast trades in the eastern North Pacific.

Wind records at SONGS from 1981 through 1986 are shown in Vol. VI-3 (Reitzel et al, 1987) along with the distribution of the wind direction (wind roses) for summer and winter seasons. Noteworthy are the following:

1. The period between December 19, 1982 and March, 1983, are characterized by the frequent occurrence of winds with speeds greater than 5 m/sec.

2. Winter winds are mainly from the north, while summer winds can come from a semi-circle direction from the west. Because winds blow mainly from upcoast, there are often chronic upwellings on the coast.

4.6 Runoff and Fine Sediments

The principal supply of fine sediments (silt and clay sizes of grain diameter < .062 mm, $\phi > 4$) to the nearshore shelf off San Onofre comes from suspended grains carried in the runoff of creeks and rivers in the region. This runoff is highly episodic, with nearly all the total volume of stream discharge coming from flood periods of a few days following winter rainstorms in unusually wet years. Since the total sediment load carried by a stream increases almost as the square of the discharge, the supply of sediment is even more highly concentrated in extreme events. Table 4-7, adapted from Gayman (1986), gives estimates for the supply of fine sediments from each principal source. Coastal erosion by waves, together with longshore transport in the surf zone, is the main source of beach sand on this coast. However, the table shows that coastal erosion is a less important source of fine sediments than local streams.

Figure 4-26 shows the history of rainfall at San Onofre from mid-1971 through 1986, and Figure 4-27 shows the annual runoff (the volume of discharge divided by the area of the watershed) for all the major streams between Dana Point (about 20 km upcoast from San Onofre) and Oceanside (about 30 km downcoast). In the series of comparatively dry years from 1970 through 1977, runoff was a very small and variable fraction of rainfall, which went mostly to evaporation, transpiration, or groundwater storage in the watersheds. In the more rainy times since 1977, runoff became much more uniform among watersheds and rose to a higher fraction of the rainfall, exceeding one-third in some years.

The yields of total sediments and fine sediments from San Juan Creek were found directly by the USGS through regular measurements of total suspended material in the discharge with grain-size analyses of this material from time to time. Table 4-8 shows the annual discharge and yields for San Juan Creek for 1974-84.

TABLE 4-7

SUPPLY OF FINE SEDIMENTS TO THE SEA
(Thousands of metric tons)

WATERSHED	MAX. DAILY	MAX. ANNUAL	11-YEAR TOTAL 1974-1984
San Juan Creek and tributaries (500 km^2)	350	850	1100
San Mateo Creek and San Onofre Creek (350 km^2)	200	200	450
Las Flores and Other Creeks (200 km^2)	100	150	300
Santa Margarita and San Luis Rey Rivers (3400 km^2)	250	900	3900
Erosion of Coastal Gullies	50	150	300
Erosion of Sea-Cliffs	50	100	200
Sewage Outfall	.02	5	50

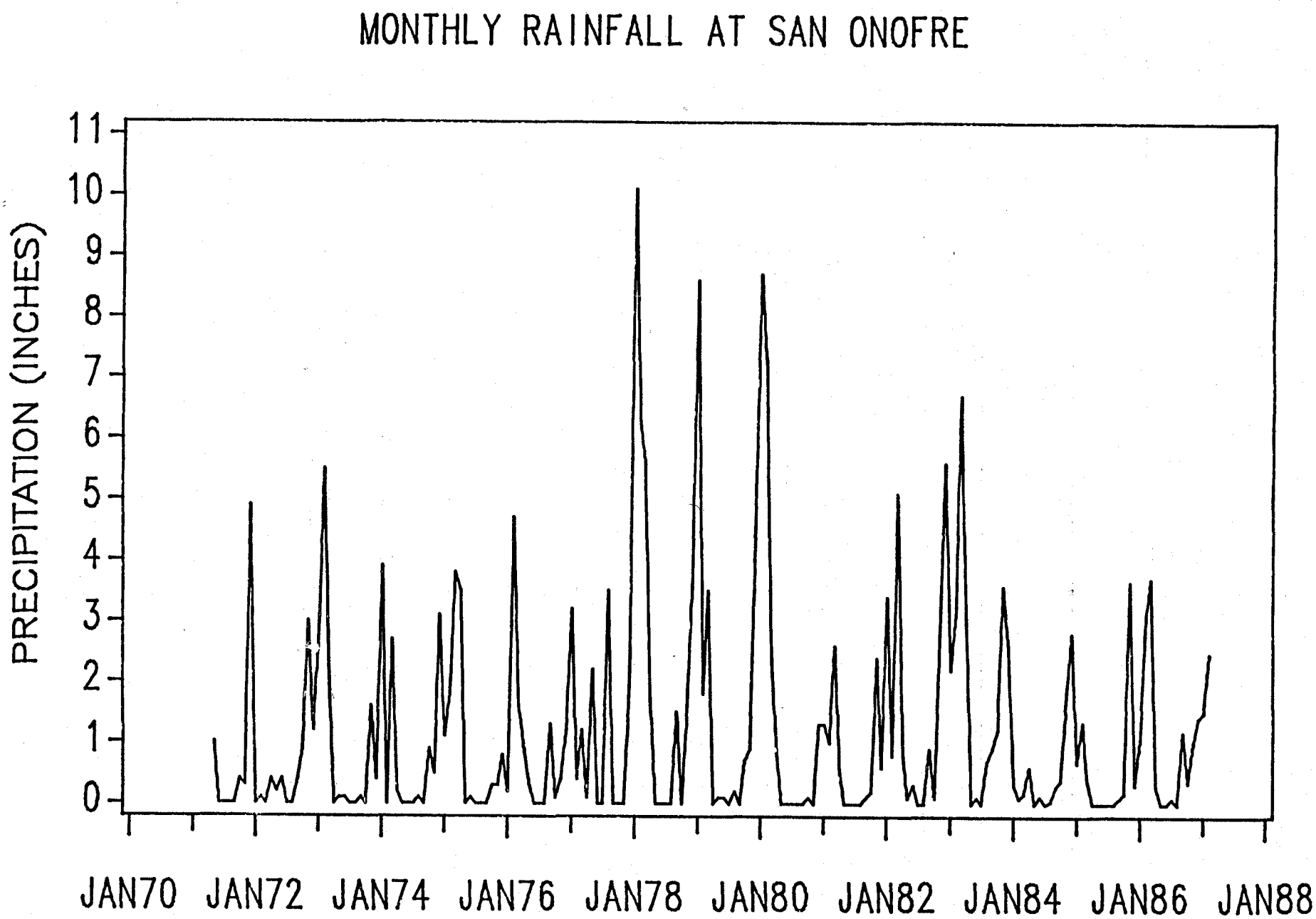

Figure 4-26. Monthly mean of rainfall at San Onofre

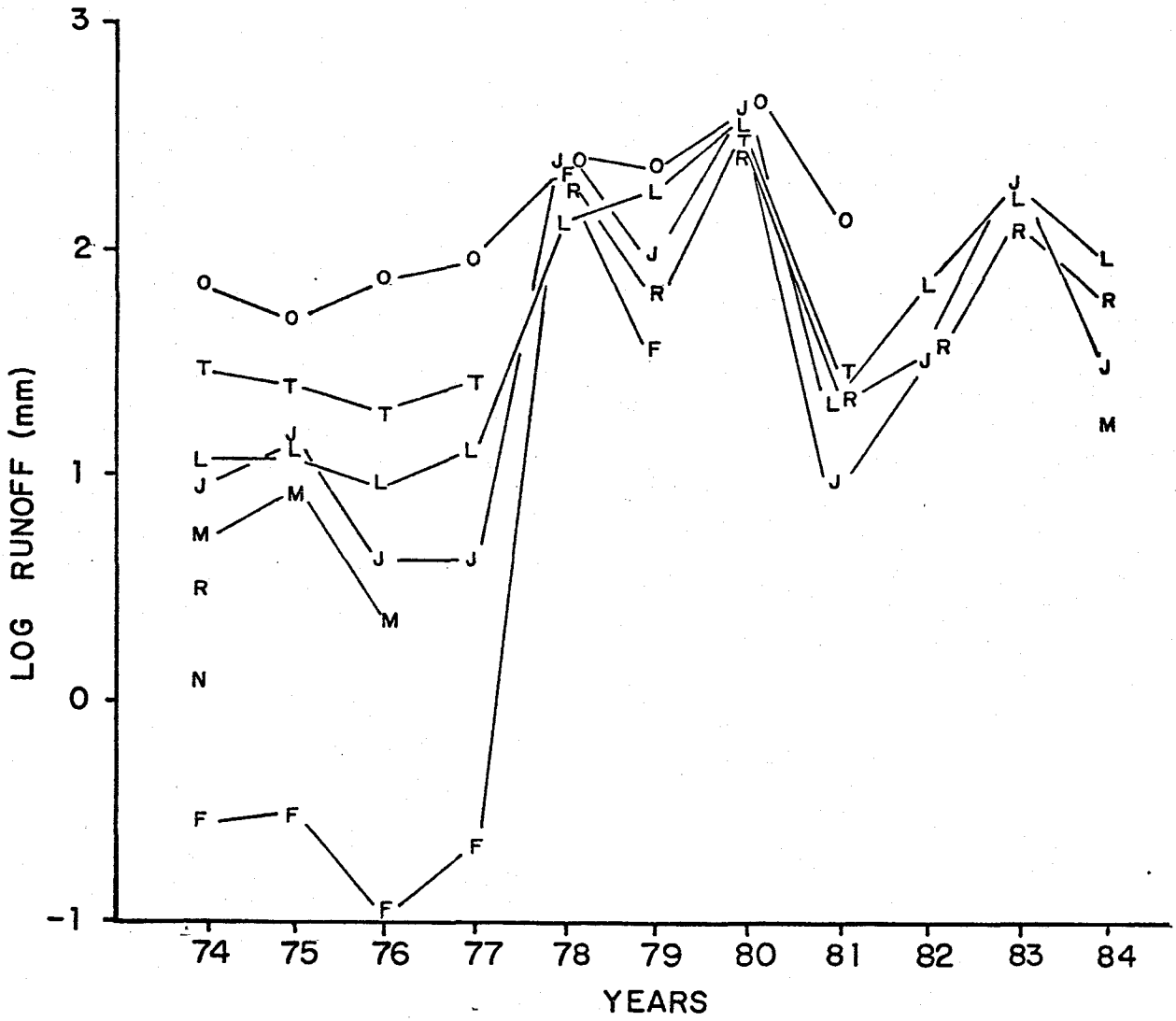

O = Oso Creek
T = Arroyo Tribuco
J = San Juan
M = San Mateo
N = San Onofre
F = Las Flores
R = Santa Margarita

Figure 4-27. Annual runoff for major streams between Dana Point and Oceanside

TABLE 4-8

ANNUAL DISCHARGE AND YIELDS
(Year by Year Records from San Juan Creek)

SAN JUAN CREEK (300 km^2)	ANNUAL RUNOFF (centimeters)	ANNUAL TOTAL SEDIMENT SUPPLY (thousands of metric tons)	ANNUAL FINE SEDIMENT SUPPLY (thousands of metric tons)
1974	0.9	0.5	0.4
1975	1.4	2.1	1.2
1976	0.4	0.2	0.1
1977	0.4	0.2	0.2
1978	28.1	661.0	496.0
1979	10.1	48.0	39.0
1980	43.8	877.0	41.0
1981	0.9	0.6	0.6
1982	3.6	16.2	11.4
1983	23.0	209.0	98.0
1984	3.1	2.0	1.3

The years in this table and in Figure 4-27 are so-called water years, beginning on the previous October 1, so that water year 1978, for instance, includes the whole winter of 1977-78. Sediment loads were measured only occasionally, if at all, on other streams, and the estimates for other streams in Table 4-7 are made by extrapolating yields per unit area of watershed from San Juan Creek. Since runoff becomes fairly uniform in wet years, and sediment yields per unit area show fairly high log-log correlations with runoff, this method is adequate for approximating annual yields in wet years. San Juan Creek brought down 575 thousand metric tons of fine sediment from 300 km^2 of watershed in the water years 1978-80, so we can estimate that all the creeks north of San Onofre brought down about 1500 thousand metric tons from 850 km^2 of generally similar watershed in 1978-80. Similarly, we can estimate that all the creeks north of San Onofre brought down about 250 thousand metric tons of fine sedments in water year 1983.

The results of an extensive program of sediment coring off San Onofre are summarized in a series of maps by Barnett et al (1986). The bulk of most sediments beyond the surf zone off San Onofre is made up of grains with sizes not very far from the sand-silt boundary (.062 mm) on either side, and the silt-clay percentage is a sensitive indicator of changes that are directly measured in grain-size analyses. Figure 4-28 shows contours of silt-clay percentage on the 7.6 m isobath, on a plot of time and distance downcoast from SONGS. Figure 4-29 shows the same for silt-clay percentage on the 18.3 m isobath, about 700 m offshore of the San Onofre kelp and the end of the diffuser lines.

At 7.6 m, the most notable events (aside from a single aberrant point at X=7000 m, 1983) are the rises above 30 % around X=2000 m in 1980-81 and 1983-84. The rise to 38% in the spring of 1980 was accompanied by a marked decrease in the sorting of sediments near San Onofre, beginning at stations 2.5 km upcoast in March and spreading to stations more than 3 km downcoast in May. At 18.3 m, there was a

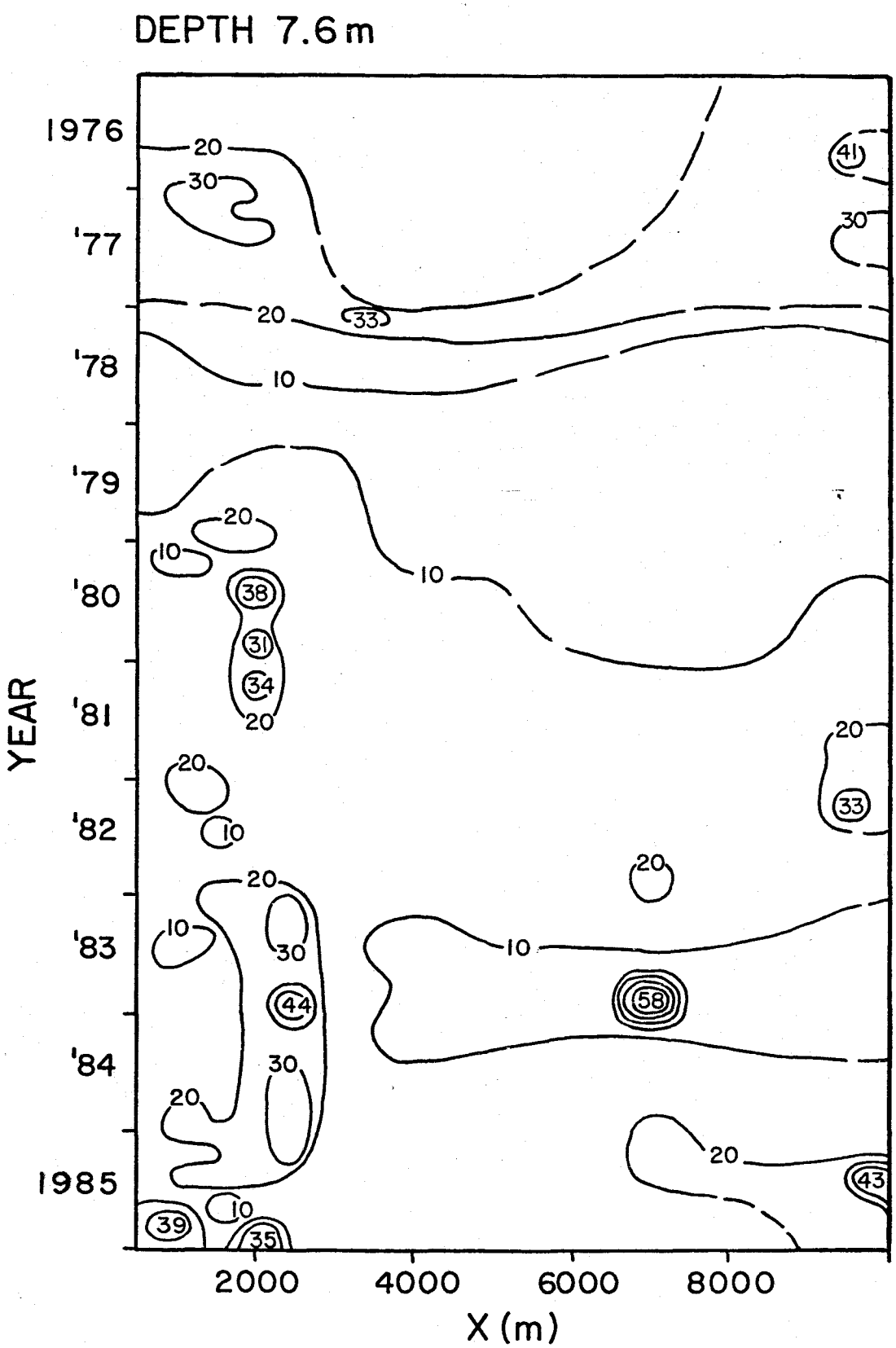

Figure 4-28. Percentage of silt and clay in sediments at 7.6 depth of water, 1976-1985

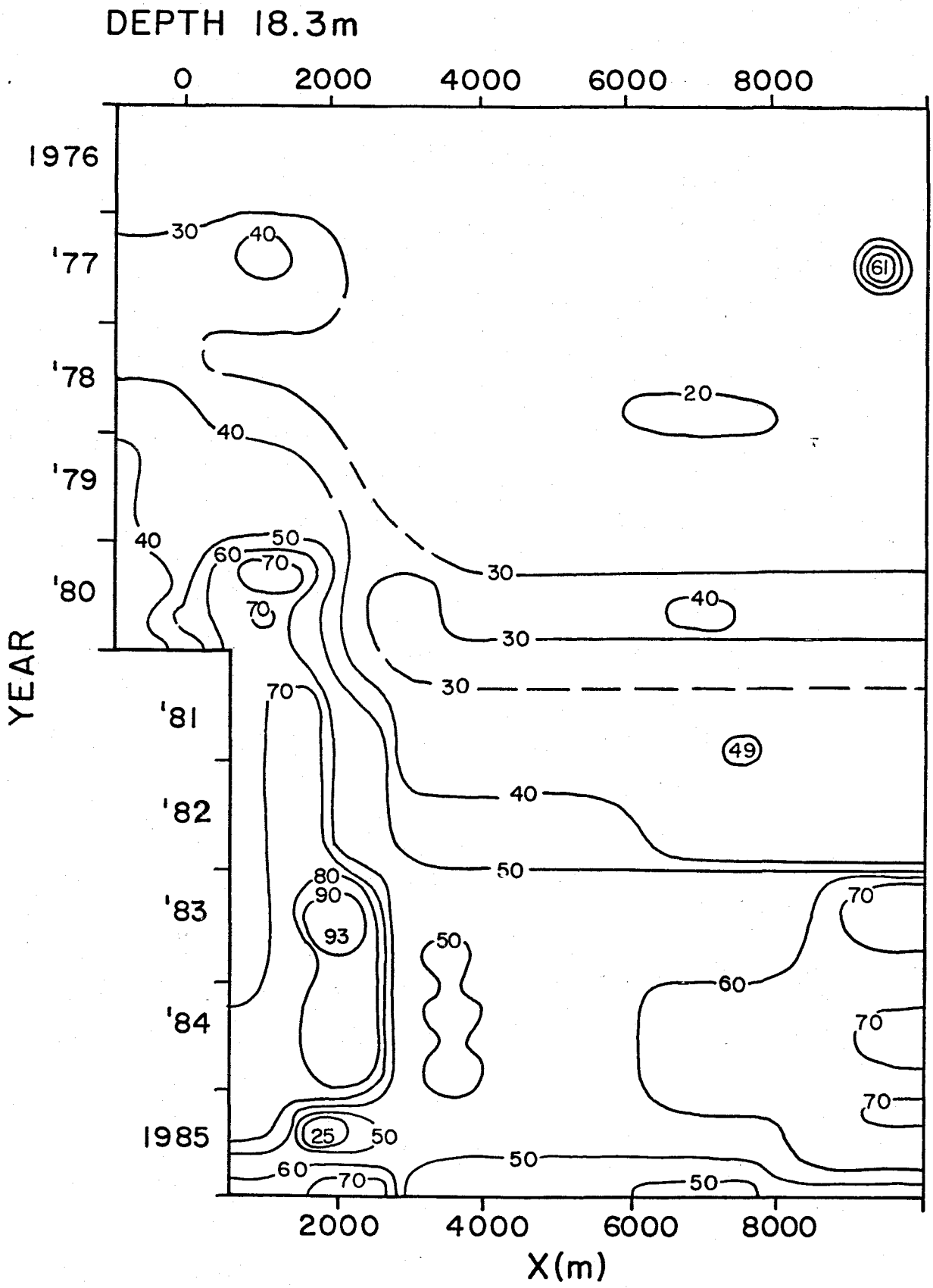

Figure 4-29. Percentage of silt and clay in sediments at 18.3 depth of water, 1976-1985

striking overall increase in silt-clay percentage over the years from generally below 30% before 1983 to generally above 50% after 1982. As at 7.6 m, there were notable local increases at X=1000-2000 m, a rise to about 70% in 1980 that generally persisted afterward, and a further increase above 80% through 1983-84.

These matters are considered further in Vol. II-2, in the chapters on the effects of SONGS construction and of the sand-release of 1984-5. Speaking here of natural changes only, we note that the changes in sorting at 7.6 m indicate that the 1980 increase in silt-clay percentage was due to an influx of fines from upcoast. The increase could be generally due to the high runoffs beginning in 1978, arriving with a delay of a year or two, or from the runoff of 1980 in particular, arriving after a few months, like the increases in 1983 which are clearly associated with the runoff of the same year.

The overall increase in silt-clay percentage at 18.3 m in the region downcoast of San Onofre can probably be attributed to the ending of the long cycle of dry years from 1970 through 1977, during which fines were sinnowed and dispersed further offshore by waves without being replaced by runoff. The region from about 3 to 6 km downcoast from San Onofre lies off a very small local watershed midway between San Onofre and Las Flores Creek. The pattern of increases at 18.3 m after 1982 shows a minimum in this region, with evidence of an influx of fines from the north (upcurrent) and a smaller influx from the south. The reason why silt-clay percentage at both depths tends to be highest around X=2000 m is not evident.

5. SUMMARY OF MAJOR OCEANOGRAPHIC EVENTS

The ocean environment at SONGS is marked by the decline and return of density stratification resulting from the varying temperature difference between surface and bottom waters (see Section 4.1). Summer is generally characteristic of highly stratified waters. That is, the temperature difference between surface and bottom waters is great. During January and February, the temperature difference is very small. At the end of March these differences start to build, and restratification is accomplished by the end of April.

This seasonal cycle is interrupted by periods of upwelling, downwelling, wave storms, wind storms, and El Nino events. The following gives the distinctive events which occurred at the San Onofre area during the period 1981-1986:

1. In 1981, from early August until the end of October 1981 (a 3-month period), the daily mean current at San Onofre was in the downcoast direction; the average current speed was 20 cm/sec. This is an unusually long period of time without a current reversal.

2. El Nino arrived at San Onofre in September of 1982. A mass of water of low salinity and low nutrient concentration came from about 500 km offshore, from the west/southwest. This mass was succeeded in December by warmer water (16° - 17°C) equally low in nutrients. The coastal water remained abnormally warm and low in nutrients through 1983, except for two upwellings in April and May, 1983, which permitted phytoplankton blooms and a local recruitment of kelp. The decline of El Nino occurred by the spring of 1984.

3. January and February of 1983 were periods of severe winter storms, heavy winds, rain and high waves.

4. Starting with the operation of Units 2 and 3 (at the end of 1982 and the beginning of 1983), there were changes in the vicinity of

the diffusers in the biological populations (see Barnett et al, 1987; Dean et al, 1987; Schroeter et al, 1987; DeMartini et al, 1987) as well as noticeable increases in surface water turbidity (see Vol.II-2). There were also changes in the flow field patterns and a reduction of light level at the ocean bottom (see Vol.III-1).

5. In August and early September of 1984, the surface temperature frequently exceeded 24°C for several consecutive days. This was the warmest period since 1981. Temperatures did not fall below 22°C during this time.

6. During the summer seasons, the turbid layer near the bottom, caused by particles resuspended by waves and swells, is kept between 0 and 2 m above the bottom due to the stratification of the water column during this period.

7. A noteworthy physical characteristic of the spring and summer of 1985 was the low temperature of the nearshore water column compared to that in the two previous summers. 1983 was an El Nino summer with warm and nutrient-poor conditions in nearshore waters. 1984 was a year of record high temperatures, remaining above 22°C throughout August and September. However, surface temperatures in 1985 seldom exceeded 20°C (as in the mid-June downwelling), and overall averaged about 2°C cooler than in the previous year.

8. The major upwelling which happened in the study area during the period 1981 through 1986 was on June 25, 1985, in which both surface and bottom temperatures fell more than 7°C in less than five days, to 14°C at the surface and 10°C at the bottom. Both surface and bottom temperatures returned to values at previous levels on July 3. The second strongest upwelling in the area came on June 24, 1986 and lasted until June 28. The surface temperature dropped 5° (from 20.3°C to 15.2°C), bottom temperature 2.2°C (from 13.7°C to 11.5°C).

9. In general, the period of April, 1985 through July 1, 1985 was a time of nutrient enrichment for the kelp beds. This condition changes sharply after July 1 when bottom temperatures rose above 14°C and essentially stayed there until March 1986. This is more or less a seasonal shift from a nutrient-rich productive period (April-July) to a period of reduced nutrient availability and decreased productivity after July 1, 1985, and continuing through the end of the year.

10. In August of 1986, bottom temperature remained relatively high with respect to the expected temperature for this time of the year. Both surface and bottom temperatures were about 17°C and remained there for the rest of year. The surface water temperature was also warmer than expected. This event was a condition reminiscent of the El Nino of 1982-1984.

Table 5-1 is a schematic month-by-month calendar of notable oceanographic events from mid-1981 through 1986, using capital letters to designate the most important events and small letters for secondary events. Each letter represents a single event. Retyping the same letter in the cell is an indication of the number of occurrences of the event during the month. All events of this kind lie on a continuum from minor to extreme, and the criteria for selecting important events have to be somewhat arbitrary. This calendar can be used for a quick overview of the history, but is certainly not an exhaustive catalog of events, nor an authoritative guide to their significance.

TABLE 5-1

OCEANOGRAPHIC EVENTS

	J	F	M	A	M	J	J	A	S	O	N	D
1981	•					u	u				u b	w
1982	s s w		S s w	u b W	u w				N→ W		s s	S w
1983	s	S w w	s R W w	u s	u	u		D W W	D s w		s s	
1984	s		w	U S w w w		u		D	D		←N w	s s
1985			s w w	B	u B	U B	u B	u d	u		S	w
1986	s s	S S W	s s w W	u s	u B w	U B s	U B	u	u B d			

U,u upwellings

D,d downwellings

B,b phytoplankton blooms

S,s windstorms

W,w high waves

N→ ←N beginning and end of 1982-84 El Nino

R high runoff

REFERENCES

Barnett, A.M., 1986. Historical Record of Grain Size and Organic Carbon Data. Report submitted to the MRC, May 2, 1986.

Barnett, A.M., 1987. Monitoring Studies on Ichthyoplankton and Zooplankton. Final Report submitted to the MRC, October 8, 1987.

Barnett, A.M., 1987. San Onofre Nuclear Generating Station Monitoring Studies on Mysids and Soft Bottom Benthos. Final Report submitted to the MRC, November 30, 1987.

Dean, T.A., L. Deysher and F. Jacobsen, 1987. The Effects of the Discharges from the San Onofre Nuclear Generating Station on the Giant Kelp. Final Report submitted to the MRC, April 30, 1987.

DeMartini, E.E., 1987. The Effects of Operations of the San Onofre Nuclear Generating Station on Fish. Final Report submitted to the MRC, December, 1987.

Dixon, J.D. and S. Schroeter, 1987. Studies of Benthic Organisms in Kelp Forests Near the San Onofre Nuclear Generating Station, 1980-1986. Report submitted to the MRC, June 17, 1987.

Gayman, W., 1986. Investigation of the Supply of Fine Sediments to Nearshore Water in the SONGS Region. Report submitted to the MRC on August 15, 1986.

Lentz, S.J., 1984. Subinertial Motions on the Southern California Continental Shelf. Ph.D Thesis, Scripps Institution of Oceanography.

Lentz, S.J., 1985. The Spatial Coherence of Motion in the Ocean Offshore of the San Onofre Nuclear Generating Station During the Winter. Report submitted to the MRC, August 9, 1985.

Lynn, R.J., K.A. Bliss and L.E. Eber, 1982. Vertical and Horizontal Distributions of Seasonal Mean Temperature, Salinity Sigma-T, Stability, Dynamic Height, Oxygen, and Oxygen Saturation in the California Current 1950-1978. Calcofi Atlas No. 30, edited by A. Fleminger.

Reitzel, J., H. Elwany, R. Erdman and K. Zabloudil, 1987. SONGS Physical and Chemical Oceanography Program. Draft Final Report, Vol. VI-1 (Data Bases: Organization, Access and Contents), Vol. VI-4 (Instrumentation), Vol. VI-3 (Summaries of Data), Vol. III-1 (Statistical Analyses: Estimated Physical Changes Due to SONGS), Vol. II-2 (Synoptic Studies of the Plume of SONGS Units 2 and 3, and Effects of Construction and Sand Release), Vol. V-2 (The Relation of Disolved Nitrate to Temperature Off San Onofre), and Vol. IV-2 (Kelp Mapping Survey). Report submitted to the MRC, 1987.

Reitzel, J., H. Elwany, R. Erdman and K. Zabloudil, 1987. Measurements of Suspended Particles Utilizing Pump System. Report submitted to the MRC, November 9, 1987.

Schroeter, S.C., J. Dixon and T. Dean, 1987. Effects of the Operation of SONGS Units 2 and 3 on Patterns of Kelp Recruitment in the San Onofre Kelp Forest. Report submitted to the MRC, July 3, 1987.

Winant,C.D., and W. Bratkovich, 1981. Temperature and Currents on the Southern California Shelf: A Description of the Variability. J. of Phys. Oceanography, Vol. 11, No. 1, pp. 71-86.

APPENDIX A

CURRENT MEASUREMENTS DATA SET

Between 1977 and 1986, current meter measurements were made in the shelf waters off San Onofre. Two types of current meters were used to obtain the data. Between 1977 and 1985, a vector measuring current meter called the Davis-Weller meter was used. It was developed at the Scripps Institution of Oceanography in the 1970's and consists of two pairs of orthogonal, 5-bladed propellors which were designed for a nearly perfect cosine response. This ensures that under an energetic wave field, the orbital motions are averaged out properly and small mean currents can be measured with confidence. The instruments containd a flux gate compass but were not vector averaging. The meters were moored on Sheldon Spar buoys that prevented rotation of the meter around the vertical axis. In other words, the meters were held in position by the mooring and the information regarding the bearing angle of the propellors was measured by the flux gate compass.

In 1985, a one-year transition to the S4 electromagnetic current meter (manufactured by Inter-Ocean in San Diego) began. The S4 is now widely accepted in the oceanographic community as is the Davis-Weller meter. The principal advantages of the S4 are its ease of handling in the field, lower maintenance, ability to retrieve data in the field, and immediate re-deployment (the turnaround time for the S4 is a few

hours whereas for the Davis-Weller, it was many days). A more complete discussion of the instrumentation is found in ECO-M's Report Volume VI-4 (1987).

Timeline plots of the available current data are presented year by year in Figures 1 and 2. The station numbers, whose locations are shown on the map at the top of the figures, are given with the depth of the measurement along each timeline.

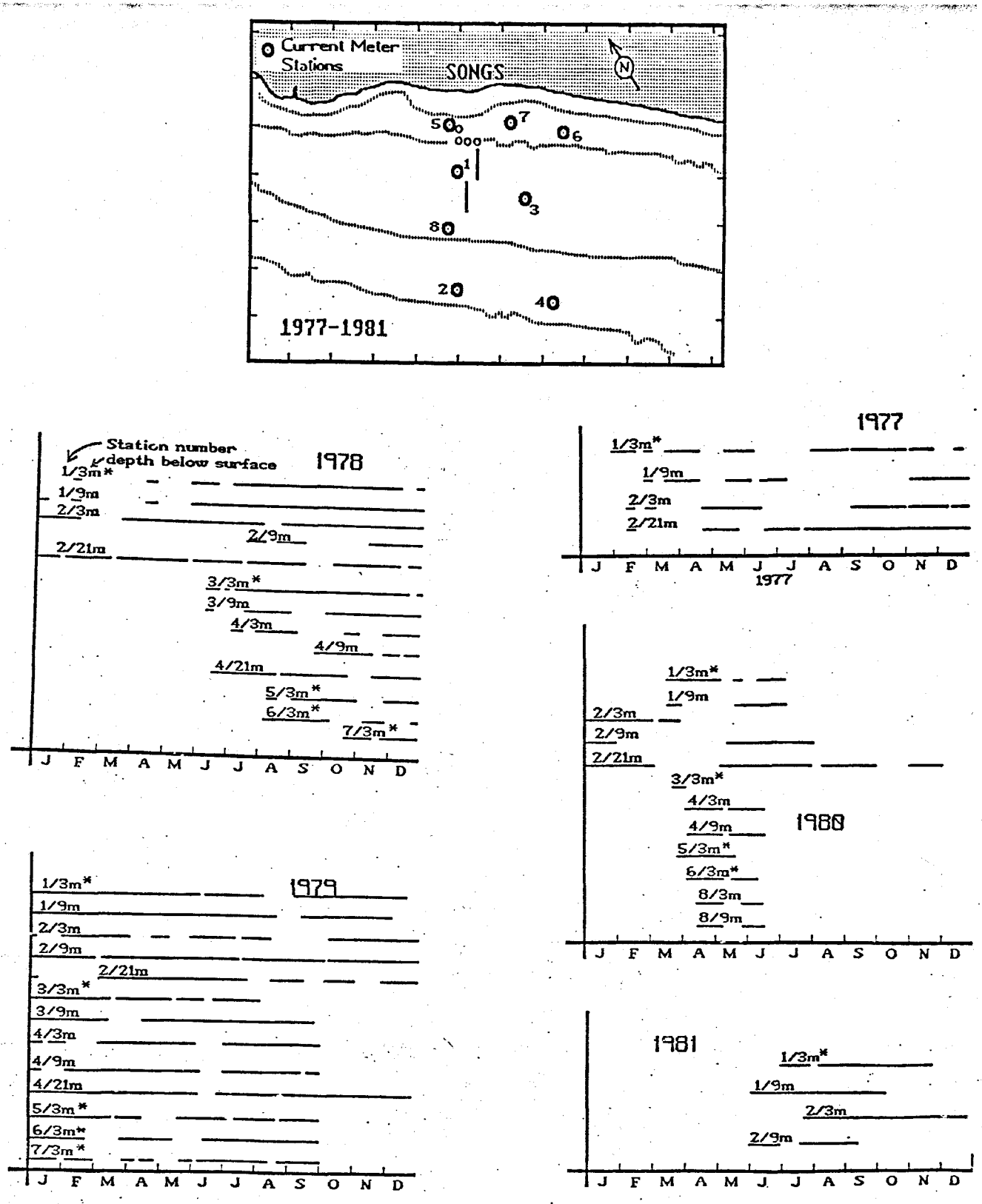

Figure 1 Current meter data measured on the shelf off San Onofre between 1977 and 1981. Depths below the surface are given with respect to MLLW. The asterisks following the station number/depth labels denote those measurements were used in forming the composite time series described in the text.

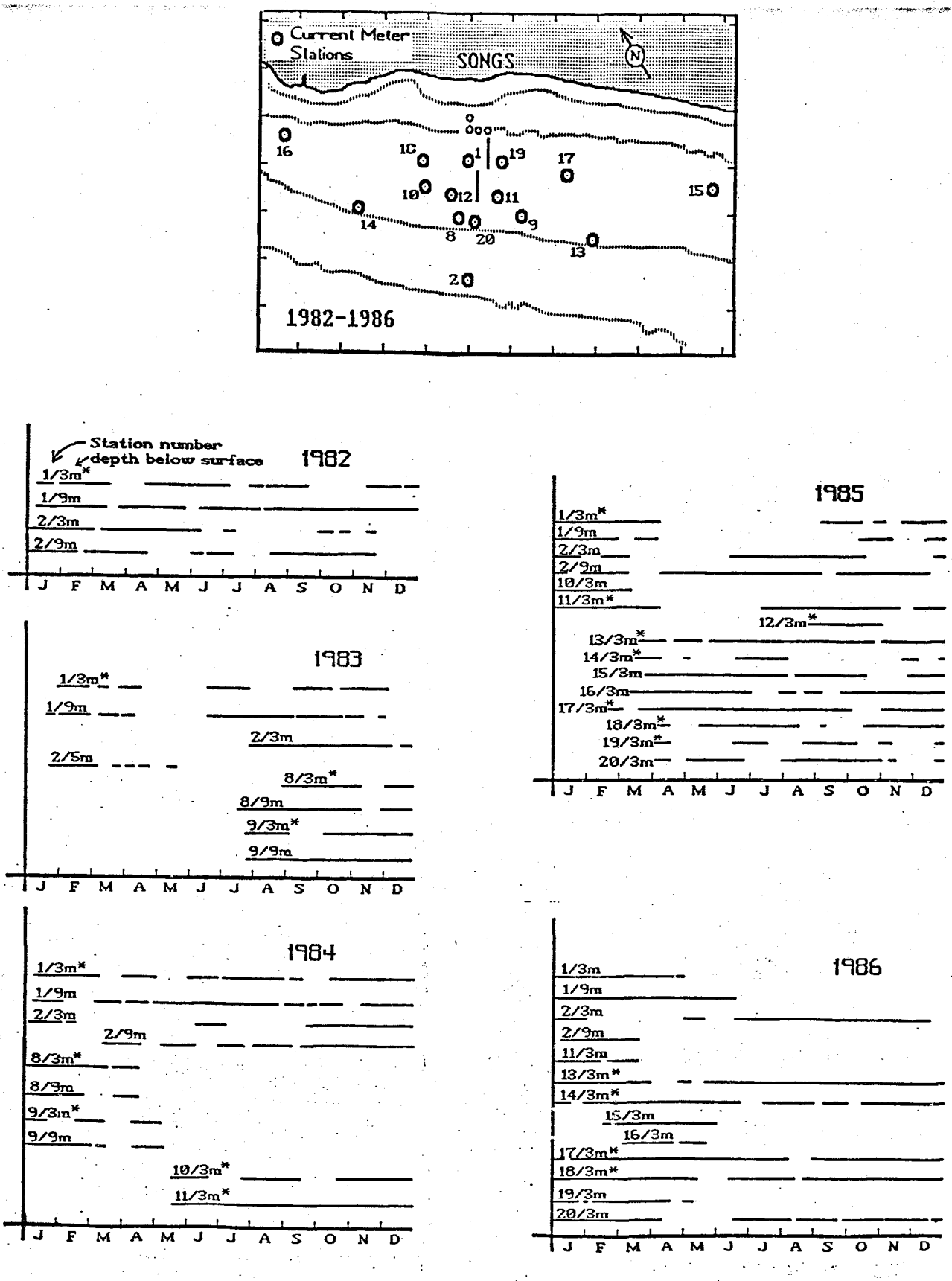

Figure 2 Current meter data measured on the shelf off San Onofre. between 1982 and 1986. Depths below the surface are given with respect to MLLW. The asterisks following the station number/depth labels denote those measurements were used in forming the composite time series described in the text. The intense measurement campaign that began in February 1985 and lasted through 1986 is often referred to as part of the plume monitoring program, a program designed to study the near field circulation patterns and associated light and temperature effects due to the operation of SONGS.